Camera System Engineering Design for the Deep Underground Neutrino Experiment

A thesis submitted in partial fulfillment of the requirement
for the degree of Bachelor of Science in
Physics from the College of William and Mary in Virginia

By

Ridge D. Poole, Ashley K. Yoon, William Z. Fesjian

_____

Advisor: Professor Jeffrey K. Nelson

_____

Professor Irina Novikova

_____

_____

Williamsburg, Virginia
May 2018

Contents

Acknowledgements

We would like to thank the Physics Department for being so supportive of our research throughout this 2017-2018 school year, especially Professor Jeffrey Nelson, whose advisement through this entire project was helpful and generous.

We would also like to thank our family and friends who have been kind to us and supported us our entire lives.

List of Figures

List of Tables

Abstract

Over the past two semesters, our team worked on engineering a sensor system that would employ a high grade professional camera along with various optical components. The designed system is to be used for the observation of a neutrino detector located in South Dakota at the Sanford Research Facility. This detector is an essential part of the Deep Underground Neutrino Experiment, which is an international collaboration with the intention of advancing neutrino science and proton decay studies. The goal of our project was to be able to collect and process high resolution internal images of four cryogenic liquid argon (LAr) chambers (cryostats) using a remote controlled, high frame rate camera system. Our camera system would act as a monitoring arrangement in which we have access to real time, full-frame viewing inside the cryostats of the Far Detector. We tested several prototype designs for this project with the idea of working out which would be the superior option in terms of ease of machining, ease of implementation, and production of quality images with an extensive field of view. Our final design expanded on the more successful prototype, which consisted of a plano-convex “fisheye” lens and a bi-concave lens that sits behind the fisheye lens. These lenses would reside within a lens tube mounted inside one end of an aluminum pipe, while our camera would be mounted at the opening of the other end. This paper details our process from identifying the requirements of our project to integrating the work of each individual within the team.

Chapter 1

Background and Introduction

1.1 The Deep Underground Neutrino Experiment *(Ashley, Ridge, Will)*

The Deep Underground Neutrino Experiment (DUNE) is a large project located in the United States that will use advanced particle detection technology to conduct research in neutrino science and proton decay studies. It operates on an international level, in that over 1000 scientists from different institutions worldwide have contributed to the project. DUNE utilizes two massive underground detectors; one (the Near Detector) housed at the Fermi National Accelerator Laboratory (Fermilab) in Batavia, Illinois, and the other (the Far Detector), roughly 1,300 kilometers to the west, housed underneath the Sanford Research Facility in Lead, South Dakota.

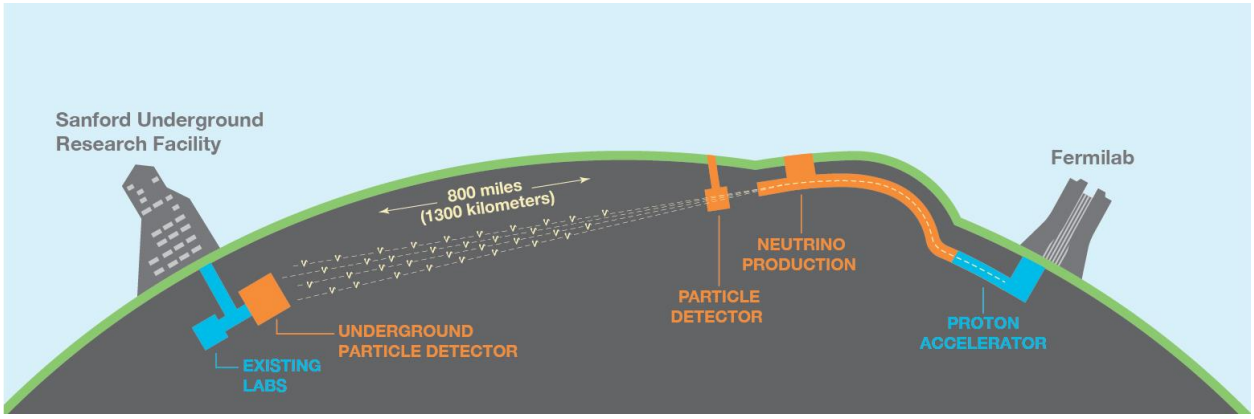

Figure 1.1: DUNE's Two Neutrino Detectors are shown above--the Near Detector at Fermi National Accelerator Laboratory (Batavia, Illinois) and the Far Detector at Sanford Underground Research Laboratory (Lead, South Dakota). Neutrinos are to be generated at Fermilab and then passed through 1,300 km of Earth in hopes of observing their behavior at the Far Detector.

DUNE's Near Detector will be built at Fermilab, which is a few hundred meters downstream of a neutrino source and is currently in its design stage [1]. Its primary function will be to characterize the neutrino beam passing through. This will allow scientists working on the project to better understand the subsequent data collected at the Far Detector. One of the prominent design ideas for the Near Detector is that of a straw-tube tracking detector and electromagnetic calorimeter, which would reside within a large dipole magnet [2]. The data collected from the Near Detector will be utilized in the study of neutrino nuclear interactions.

The Far Detector, which will be located at the Sanford Underground Laboratory (SUL), has plans of being built 1,475 meters underground in order to shield the sensitive device from cosmic rays. Thus, only neutrinos and infrequent high energy muons would be allowed to reach the detector [3]. At SUL, there are existing labs and infrastructure at various depths, including the level at which the DUNE detectors will be constructed. The Far Detector will become its own wing of the lab complex and will consist of two different designs: one using single phase technology, and the other using dual-phase technology. The detector will consist of four cryogenic modules using Liquid Argon Time-Projection Chamber (LArTPC) technology (highlighted in yellow in Figure 1.2 below; detailed in Figure 1.3 below). Each cryostat will be 18 meters high by 19 meters wide by 66 meters long [4]. The modules will be filled with a total of 68,000 tons of liquid argon held at a temperature of 89.15 K (-184°C). This breaks down to 17,000 tons of LAr per chamber [1]. Once completed, they will be the largest time projection chambers ever built. The largest LArTPC to date is the ICARUS detector at Laboratori Nazionali del Gran Sasso in Italy, which held a total of 760 tons of liquid argon and was recently shipped to Fermilab [6]. In total, the DUNE will consist of a more massive and capable detector (with the generation of an exceptional neutrino beam) than that of any previous neutrino detection experiments (such as the NOvA Neutrino Experiment [7] and the MINERvA Neutrino Experiment [8]).

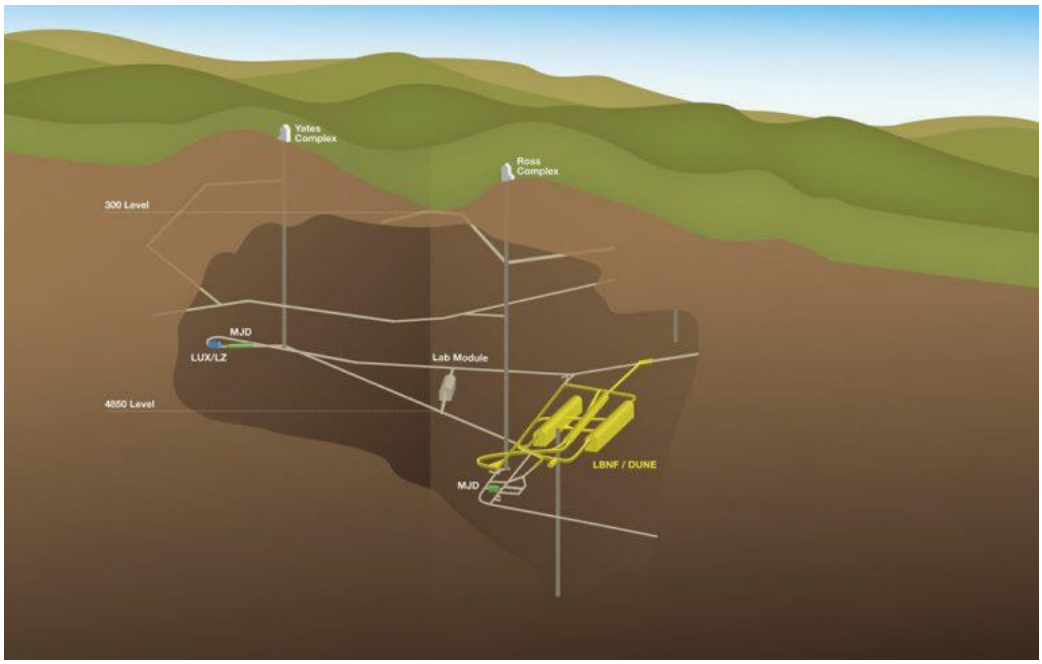

Figure 1.2: Pictured here is the Sanford Underground Research Facility in Lead, South Dakota. Mine shaft elevators are used to reach the extreme depths of the existing labs and the location where the DUNE's cryostat tanks are to be built.

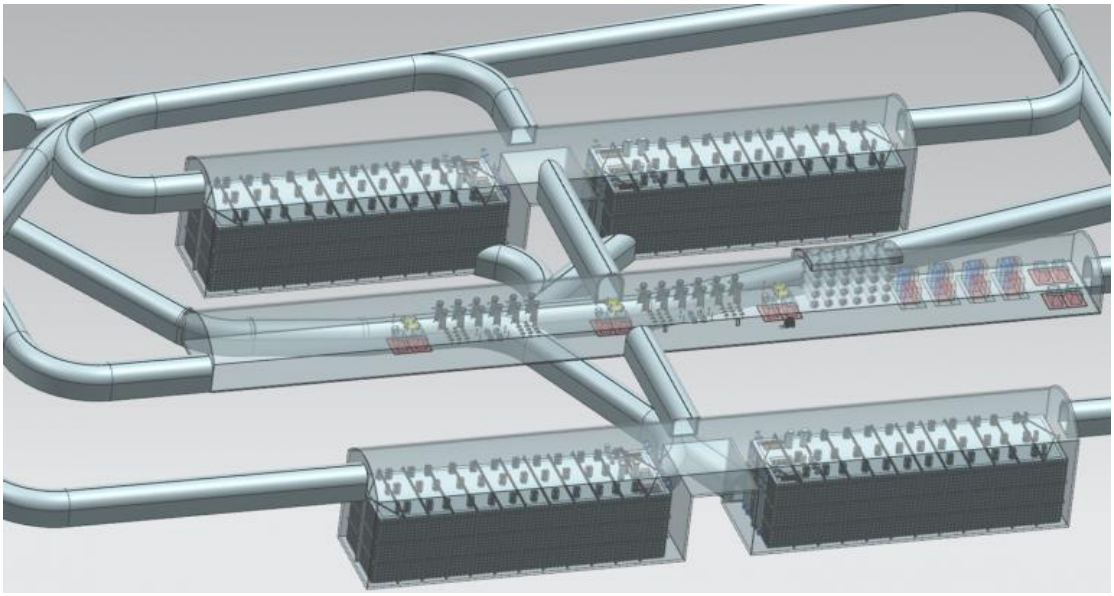
Figure 1.3: This is a more detailed model of the cryostats of the DUNE Far Detector. There will be four LArTPC tanks in total, holding 68,000 tons of the liquid argon target for the experiment.

The Far Detector will, in part, be a design evolution of both the ICARUS detector and the MicroBooNE detector (the largest LArTPC in the U.S.), which are both single-phase designs. Single-phase designs apply a series of parallel wire-planes that produce a three dimensional

image of particle tracks created by neutrino interactions [1]. There are several ProtoDUNEs, one which will, in late 2018, test this advanced single-phase technology to be employed by the completed Far Detector. The other will test dual-phase technology, which instead of using wire planes for signal readout, use a collection anode. This design also makes use of an electron multiplier to amplify the signal [9]. The two 800-ton prototypes are located at the CERN Neutrino Platform and will be used to help inform scientist and engineers of the appropriate technology choices for the completed detector [1].

A smaller single-phase LArTPC prototype, located at Fermilab and tested in early 2016, is detailed below in Figure 1.4. The image shows the anatomy of these chambers and the tested technology to be used at the Far Detector. Inside the cryostat, an electric field (up to 185 kV) is applied to create and facilitate electron drift. As shown, the walls of the tank are covered in cosmic ray counters (CRCs), which trigger when high energy particles (cosmic ray muons) pass through. Particles passing through the chamber will produce primary ionization, and these ionized electrons will travel through the electric field and be collected and measured by the collection system (from an anode to a cathode). Imaging is provided by wire planes (single-phase design) or a micropattern structure placed at the end of the drift path, continuously sensing and recording the signals induced by the drifting electrons, which in the prototype, travel roudly 2.2 m from one end of the detector to the other. LAr must be kept extremely pure for the electrons to drift such a distance across the time projection chamber without attaching to impurities, or absorbing interaction, for this to be successful [9]. High electric fields produce better drift for these particles.

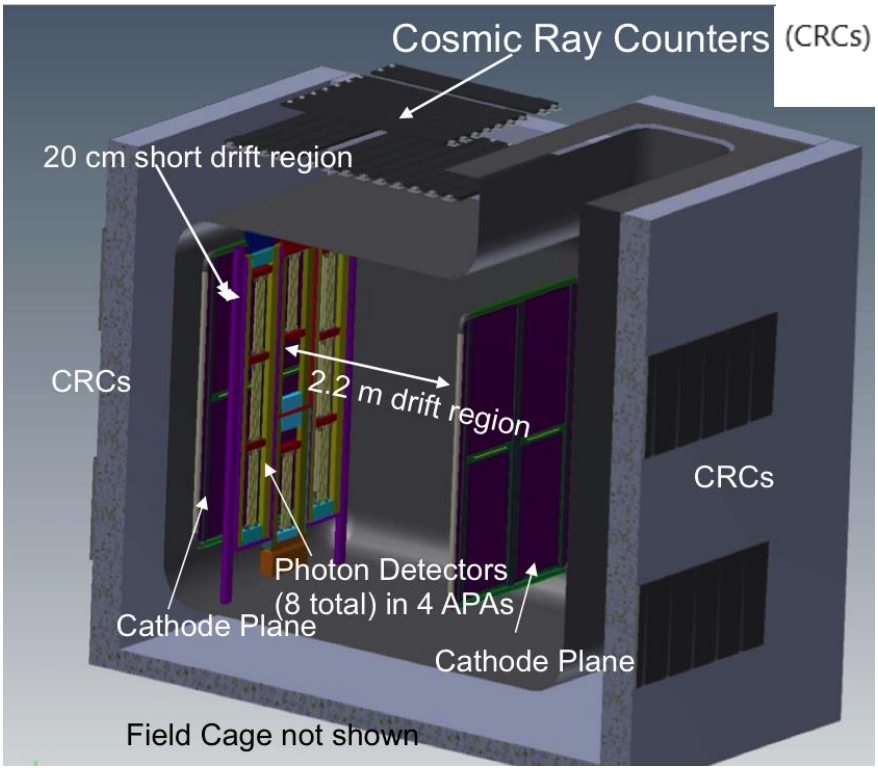

Figure 1.4: This 35 ton prototype housed at FermiLab will test many aspects of the DUNE single-phase TPC, including the FR4 field cage construction, the gaps between modules, the wrapped wire planes, the light guide style photon detection system, cold ADC ASIC in the readout electronics, and the development of triggerless DAQ operation [10].

The DUNE is not a single-purpose experiment as it incorporates multiple missions in the field of physics [3]. The first, and most obvious objective of the DUNE is to monitor the interactions of the neutrinos, which are sent via the beam generated by the LArTPC at Fermilab. Neutrinos are the most abundant particles in the universe, with trillions passing through the earth (and throughout the cosmos) every second. It is believed that during the formation of the universe, equal parts of matter and antimatter were created; but for now, ordinary matter has dominated. There are theories suggesting that neutrinos could have had a role to play in the winning out of this matter over antimatter. Henceforth, this experiment will put those theories to the test by comparing the properties of neutrinos and antineutrinos [5].

The second objective of the DUNE is to monitor incoming neutrinos from extraterrestrial sources. The placement of the LArTPCs deep underground shields them from the majority of cosmic radiation that could interfere with the experiment. The one particle that the underground environment will not be able to shield from is the neutrino (the target particle). Due to their weakly-interacting nature, extraterrestrial/interstellar neutrinos will inevitably be passing through

the DUNE's detectors along with the neutrino beam sent from Fermilab. Rather than discounting this as interference, scientists working with the DUNE hope to use these additional neutrinos to their advantage in the realm of astrophysics. Keeping an eye out for bursts of neutrinos from high energy events in the Milky Way galaxy could help shed light on the nature of cosmic phenomena, such as supernovae and the subsequent formation of neutron stars or even black holes [5].

The third objective for the DUNE is to observe the liquid argon target material for signs of proton decay. There are theories that the proton, one of the basic units that comprise the nucleus of every atom in the universe, is in fact unstable. To date however, all attempts at the observation of this phenomenon have failed. In theory, if proton decay were a real possibility, the particle lifetime would be extraordinarily long, possibly much greater than that of the universe's own existence. Therefore, to increase the chances of observation, one would need to observe an immense number of protons over an extended period of time to watch for any signs of decay. This is where the extreme size of the Far Detector's chambers comes into use. With 68,000 tons of argon and 18 protons per atom of argon, many of the researchers believe they have stacked the odds in their favor as much as is feasible given current technology. The entirety of the LArTPC, and every proton within, will be monitored for signs of proton decay. Should this decay be observed, an immense step forward would be made toward the identification of a General Unified Theory [1].

1.2 The Engineering Design Process *(Ashley)*

The Engineering Design Process is, much like the Scientific Method, a series of steps one would typically follow in order to analyze a problem. Unlike the system used by scientists (Scientific Method), which involves observation and experimentation, engineers employing the Engineering Design Process which attempt to find a solution to a problem. The solution engineers seek frequently involves designing the solution themselves. The design process involves many complex steps, from identifying the problem to construction and assessment of the proposed solution. Once a problem has been defined, background research is necessary to ensure requirements are met before proceeding to possible design solutions. Preliminary testing is an important component of choosing the superior solution out of design ideas. Once the

leading design has been selected, it will usually need to be developed further before prototyping can begin.

It is not uncommon for for engineers to identify problems with the selected prototype, which can complicate the flow of steps as modifications, redesign, and retesting can cycle through multiple times. This way of working is called iteration. Iteration improves the prototype and is an integral part of the process and allows for more sophisticated designs as well as a more efficient solution. Multiple prototypes are commonly sorted through for extensive design projects and they may be scale models of the actual finalized design. Like the Scientific process, the Engineering Design Process isn't a consistently linear process.

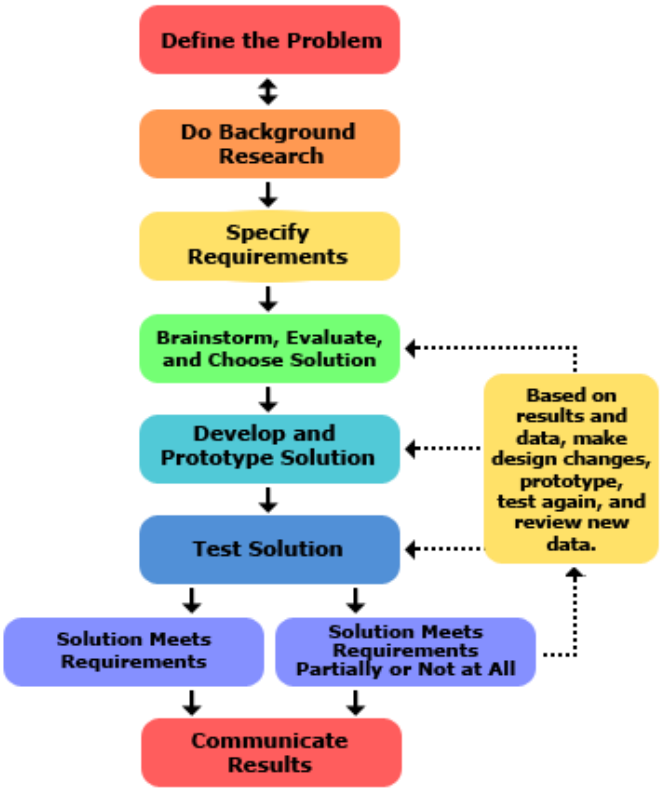

Figure 1.5: The idealized direction of flow for the Engineering Design Process

Chapter 2

Engineering Design Project

2.1 Project Foundation *(Ashley)*

The project we had been tasked with was to design and construct a camera system to be used for reliable observation inside the Far Detector's LArTPC. The purpose of the camera system is to observe spark interactions during experiments, as well as to monitor any problems arising from thermal contraction in the field cage. We wanted to be able to collect and process high resolution internal images of the chambers using a remote controlled, high frame rate camera system. This camera system would need to produce real time, full-frame viewing inside the cryostats of the Far Detector. Initial research and discussion appeared to conclude that a camera mounted to the exterior of the cryostat would be the most viable option, as thermal cycling and the extreme environment of the interior damaged the sensitive electronic components of the camera tested. The likely option given would be to mount a camera system on the exterior and have it extend through a viewport of the chamber walls, keeping the sensitive elements safe.

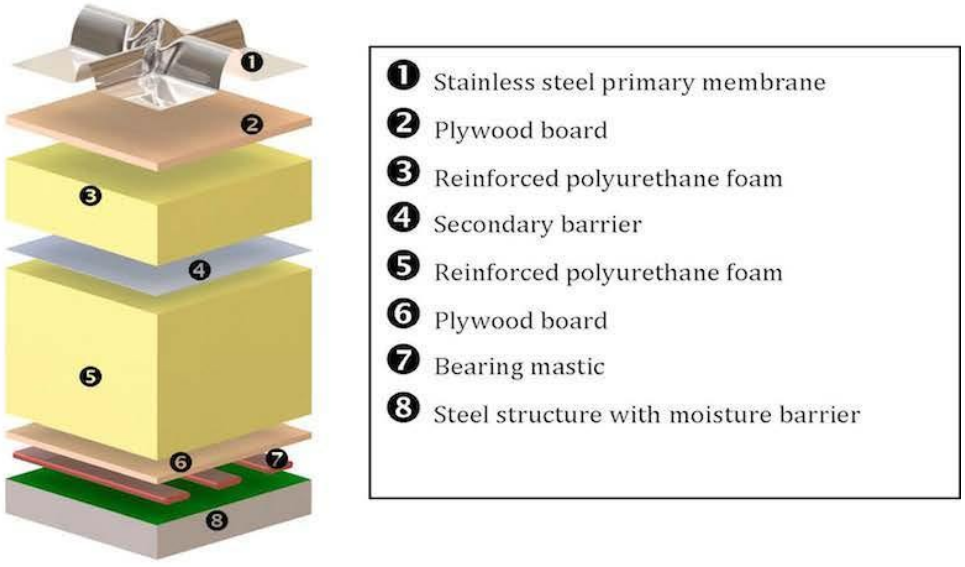

Figure 2.1: The above is a cross-sectional view of the walls that would make up the LArTPCs in the DUNE's Far Detector. The top layer here is the interior of the chamber, and the bottom is the exterior.

2.2 Previous Design *(Ridge)*

In previous prototypes of the DUNE, a cold camera monitoring system was used to observe inside the cryostat chamber. The cameras were subjected to contact with the LAr as they inspected for structural changes and sparks from the high-voltage field cage. The cameras employed were Raspberry PI units housed in a protective casing made from vacuum system components, meant to isolate them from submergent damage. The units were found to not operate reliably at cryogenic temperatures and would fail when they needed to be rebooted. This failure to reboot was thought to have come from a decrease in the bandgap size of the semiconductors within the electronics. The system would run as long as the cameras were kept on; yet, once powered off, the extreme temperatures kept them from restarting. The initial response to this problem was to implement resistive heating elements inside the casings with the Raspberry PI units, which were able to reboot the them; however, over time all six units employed failed to reboot. The heating elements proved to be insufficient for protection in the cryogenic environment. Subsequent testing showed that nearly all cameras were permanently damaged.

Figure 2.2: This image shows the six previous camera modules used as discussed. Three are face down (foreground), and three are resting on their sides (background). The Raspberry PI cameras can be seen through the glass of background units.

2.3 Design Requirements *(Ashley, Ridge)*

As mentioned above, the solution here appears to require a “warm camera” (deployed outside the liquid volume), so our plan was to test out several designs of this type. We wanted to design

a system where the cameras and sensitive hardware are kept outside of the cryostat, mounted to the exterior of the chambers, and “looking” into viewports. A tube (pipe) was implemented to house the components of our design and would extend from the exterior through roughly a meter of insulation of the chamber and into the interior of the LArTPC. Our final design would allow for full viewing of the interior of the chamber. To help withstand these low temperatures, we coated submerged components of our system in Master Bond's cryogenic shock resistant epoxy compounds--which are serviceable from 4 K and can withstand thermal cycling.

For the foundation of our design, we wanted to be able to collect and process high resolution images using a remote controlled, high frame rate camera system (minimum 1,200 fps for a resolution of 1280x1024) as mentioned in 2.1, which would also to be able to collect images at least 5 seconds in duration and to have no less than a 90° field of view. Ideally, we would want to obtain a 180° viewing angle. The camera involved would act as a monitoring system with digital zoom; through which we have access to real time, full-frame viewing, with the ability to sparsify footage and large amounts of data. Arranged below is a concise list of the aforementioned criteria and constraints:

- Camera be placed externally and view the interior of the cryostat
- 6” diameter viewports
- System must be designed to operate through a 1 m long tube (thickness of the insulation of the cryostat wall)
- 90°+ field of view (within the cryostat)
- 8” of headroom (within the cryostat)
- Camera must have a minimum frame rate of 1,200 fps (for 1280x1024 resolution)
- Camera must be able to collect images at least 5 seconds in duration
- System must be able to sparsify footage and large amounts of data
- System must be able to be controlled remotely from our computer
- Camera must have real time, full frame viewing capabilities
- System parts within the LArTPC must be able to withstand temperatures around 90 K, be stable over a temperature gradient (from 290 K), and withstand repeated thermal cycling
- Remote control of digital zoom desired

Chapter 3
Design Solutions to Previous Prototype Issues

3.1 Evaluated Prototype Designs *(Ashley, Ridge)*

One of the first, and most crucial parts of the engineering design process is to brainstorm possible solutions to the problem at hand; the three most viable options we came up with are discussed here. The first of these prototype design solutions we considered uses a convex "fisheye" lens at the base of a tunnel casing, potentially giving us a 110°-180° field of view. This design consists of a cylinder partially submerged within the liquid. The camera would be collecting images from above as it would have for the first design. This model for this design is relatively simple in composition and in implementation, as it would essentially be a one-part solution. The optical design for this system is also simple–to gather images, the camera's lens would simply have to focus on the back of the fisheye. On the electronic end of this design, software would in place to reverse the fisheye effect, giving a stream of video that appears undistorted.

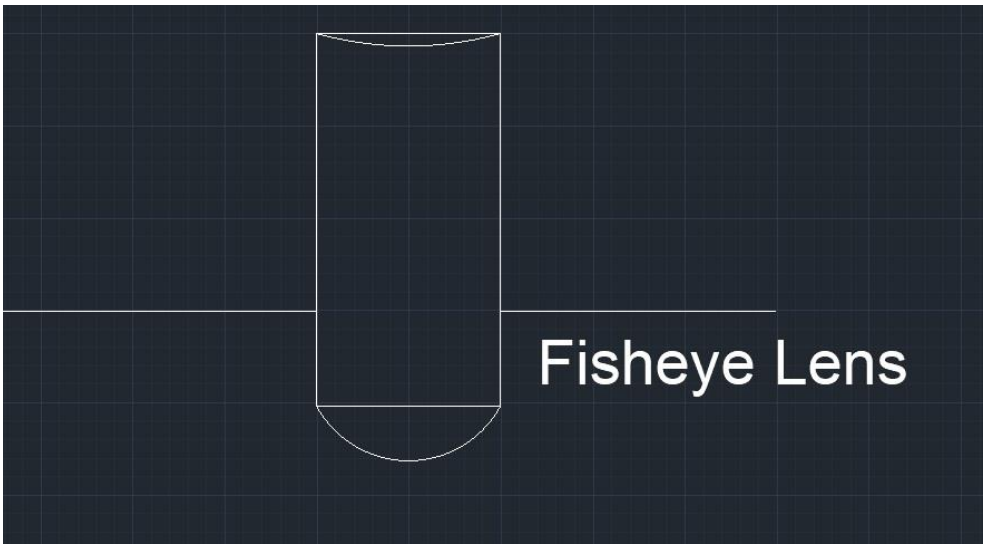

Figure 3.1: This is a simplified version of the fisheye lens design for the prototype. Again, the portion of apparatus located below the horizontal line will extend to the inside of the cryostat. *(Ashley)*

The second major prototype design considered was to implement mirrors within the cryostat or to be mounted within the tube itself. The mirrors would either be placed in an arrangement so

that the camera would be able to focus on their produced image from above (design is not pictured) or they would be mounted to a shaft extending through the tube, coming out between the lens at the base and the wall of the tube. This design could have included an array of flat or convex spherical mirrors if they were to be placed inside the cryostat itself. If flat mirrors were used, we would most likely have needed to have a system in place to rotate or move the mirror inside the cryostat remotely, so as to maximize the field of view. If convex mirrors were used, they could have possibly given the desired field of view without the need for moving the mirror inside the cryostat. We would likely have used a DC motor to rotate any of the mirrors which would be fixed within the tube.

The third design option we chose to consider was that of a fiber-optic borescope, where the end piece would be submerged the liquid. This design would allow us full customizability of the video resolution and the ability to shape the fibers of the scope in any way needed for use in the interior of the cryostat, using a hardening epoxy (straight or fisheye lens primarily). For our final design, we would need at least three feet of fibers, which is where the first limitation of the design comes in. To acquire 40 inches of fiberscope cable, at a density of 10,000 fibers, the net cost for a custom-built scope would be roughly $3,000 per unit [12]. In a scope like this, each fiber correlates to one pixel of information. Additionally, a 10,000-fiber cable would only provide a 100x100 image. We were looking for the approximate resolution of an HD camera, which means that this design has a relatively low value here. Another limitation of this particular design was the lack of information about the functionality of a borescope in cryogenic temperatures. Due to the wide availability of cheap borescopes online, we were able to purchase several for use with our prototype testing.

3.2 Optical Design *(Ashley)*

For our fisheye lens system calculations, we needed to take into account several design factors. First, there would be about 1 meter of insulation through the viewport to the chamber, which would be our cylinder length. We used this length in both our prototype design and the final design, though the diameter between the two varied (we wanted roughly a 6-inch diameter pipe for the final design, but used a 3 inch diameter pipe for our prototype). Second, we were looking for at the least, a 90^{o} viewing angle, but ideally, somewhere between 110^{o}-180^{o}, and if

possible, a 220° field of view. Utilizing a fisheye design easily placed our field of view range between 110°-180°.

Lastly, after taking the index of refraction for liquid nitrogen ($n = 1.199$), liquid argon ($n = 1.227$), and air ($n = 1$) into account, we concluded that the optical calculations worked best when the lenses were not submerged. With that, we would have about 8 inches between the end of the cylinder to the liquid argon/liquid nitrogen surface (8" headroom stated within section 2.3 Design Requirements). Our Raspberry Pi camera had a different sensor size (6.35 mm) than that of the Chronos camera (104 mm) used for our final, which became important when calculating focal lengths needed for a given field of view. Below (Figure 3.2) are the general equations we initially used to determine these variables.

Focal Length (f)

$$\frac{1}{f} = (n_l - n_s)\left(\frac{1}{R_1} - \frac{1}{R_2}\right)$$

$f = focal\ lenght$
$n_l = index\ of\ refraction\ of\ lens$
$n_s = index\ of\ refration\ of\ sustrate$
$R_1 = curvature\ on\ front\ of\ lens$
$R_2 = curvature\ on\ back\ of\ lens$

Field of View (FOV)

$$Equisolid\ Angle\ Projection$$
$$FOV = 4\tan^{-1}\left(\frac{sensor\ size}{4f}\right)$$
$$FOV\ increases\ with\ sensor/frame\ size$$

$$Focal\ length\ from\ FOV$$
$$f = (sensor\ size)/\left(4\tan\left(\frac{FOV}{4}\right)\right)$$

Figure 3.2: Equations utilized for initial optical calculations. The field of view equation above is specifically designed for use of a fisheye lens, as opposed to the usual bi-convex lens. The n_l value in the thin lens equation is assumed to be ~1.5 (N-BK7 optical glass) and the R_2 value is assumed to be infinite given the flat backing of the lens.

The table below details our calculated results found by reworking the field of view equation, for both the prototype and the final design. We were looking for needed focal lengths given a specific viewing angle. In our calculations, we specifically examined 180 degree and 220-degree angles. We chose these angles as we believed 180 degrees would be our upper limit, but also wanted to see if we could obtain a realistic result for a much more useful angle: 220 degree.

	180° FOV	220° FOV
Focal length for Prototype	1.588 mm	1.112 mm
Focal length for Final Design	26 mm	18.21 mm

Table 3.1: Focal length (f) calculations given either a 180° or 220° field of view.

Unfortunately, these focal lengths did not sufficiently move the image up the pipe and to the camera's sensor. A focal length of 1 m (estimated distance from the lens to the camera's sensor) would require a radius of curvature of 0.3 m for the optical lens (according to calculations using the thin lens equation in Figure 3.2, in which we did not take lens thickness into account), and even then, we did not obtain a viewing angle anywhere close to 180º. The sensor size would be the last variable in the FOV equation which could increase our field of view using one lens, however, we were limited by the availability of sizes produced and sold on the market, and so we determined that the optical design itself needed to be restructured.

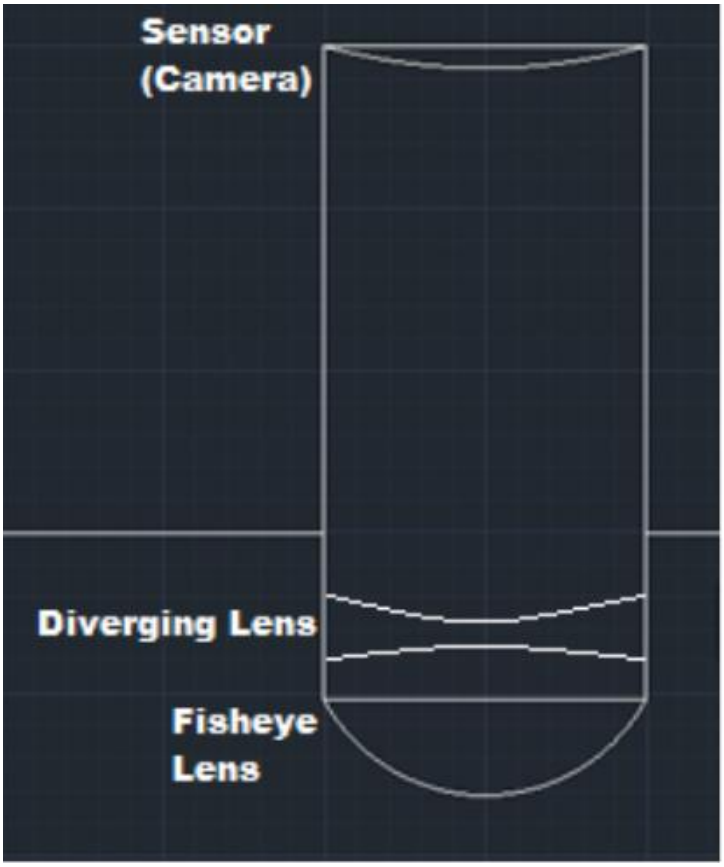

Figure 3.3: This is a redesigned version of our "fisheye" design. Here we have added a diverging (bi-concave) lens to move the location of the image up to the sensor. *(Ashley)*

We eventually worked out a design which would incorporate a system of lenses that would move the image up towards the sensor. In order to do this, we concluded that a combination of the plano-convex "fisheye" lens with a bi-concave lens, set roughly 1 mm apart for our prototype, and roughly 10 mm apart for the final design would be acceptable. This diverging lens would sit behind the converging lens, nested between that lens and its focal point, within a lens tube which would be mounted inside of the aluminum pipe. Below (Figure 3.4) are the general

equations we used to determine these distances, as well as required focal lengths for our bi-concave lenses. In our calculations, we did not take the optical properties of the camera itself into account, as we made the assumption that camera lens assembly would be similar enough to that of the human eye. Table 3.2 (also below) details our recalculated results, for both the prototype and the final design.

Location of image for fisheye

$$s_1' = \frac{s_1 \cdot f_1}{s_1 - f_1}$$

$s_1' = location\ of\ image\ 1$
$= location\ of\ object\ 1\ (LAr\ LN2\ surface\ boundary)$
$f_1 = focal\ lenght\ of\ lens$

Location of image for diverging lens

$$s_2' = \frac{s_2 \cdot f_2}{s_2 - f_2} = \infty$$

$s_2' = location\ of\ image\ 2$
$s_2 = location\ of\ object\ 2\ (object\ 2\ is\ image\ 1)$
$f_2 = focal\ lenght\ of\ lens$

Figure 3.4: Equations used for optical re-calculations

	180 FOV Plano-Convex	180 FOV Bi-Concave	220 FOV Plano-Convex	220 FOV Bi-Concave
Focal length for Prototype	1.588 mm	-0.6mm	1.112 mm	-0.12 mm
Focal length for Final Design	26 mm	-19.8 mm	18.21 mm	-10 mm

Table 3.2: Focal length (f) recalculations given either a 180º or 220º field of view, using both a plano-convex lens (converging "fisheye") and a bi-concave lens (diverging).

After discussing the pros and cons of having custom lenses machined from companies such as Custom Scientific (http://www.customscientific.com) or to have premade lenses purchased from companies such as Edmund Optics (https://www.edmundoptics.com), we decided that purchasing would not only be more time efficient but would greatly reduce the price. Partly due to time restrictions, we decided to purchase premade lenses from Thorlabs (https://www.thorlabs.com), an optical equipment company headquartered in Newton, New Jersey. Although focal lengths, lens sizes, and optical materials are restricted to availability when purchasing, we were able to find a combination which suited our needs for a greatly reduced

price to what we would have paid to have them custom made. In this case, affordability outweighed customization.

We ended up buying six lenses; four more than needed for assembly in our prototype, with the idea of using a few for submergent testing in our liquid nitrogen, in which we tested the functionality (and sensitivity) of these lenses after repeated dips to determine if a cryogenically serviceable epoxy would be needed. The affordability of these allowed us to test coated and uncoated lenses, as well as to purchase more if needed. The lenses we employed for use in our prototype have a focal of 30 mm (converging lens) and -25 mm (diverging lens) and would be set 10.2 mm apart from each other with a viewing angle of 184.5º (used with the Chronos camera). Again, due to time restrictions, we used this arrangement solely for our prototype as we did not finish building our final model, though concluded this lens combination would work on either design as long as the optical assembly could be adjusted, and the sensor size of the Chronos would be a constant. The slotted lens tube purchased from Thorlabs gave us the option of manually adjusting the bi-concave lens via the side slots without the need for a spanner wrench, giving us the ability to work this specific system of lenses into either design.

Chapter 4

Testing and Development *(Ashley, Ridge, Will)*

Testing for each design occurred in several stages and included multiple test phases per design. First and foremost, testing took place to determine the feasibility of each prototype design discussed above. Tests primarily included determining the working temperature ranges for fiber optic borescopes, testing the effects of cryogenic temperatures on mirrors and lenses, working with MasterBond's cryogenic epoxy, and testing to see if reasonable images could be obtained from the necessary distance to view through the wall of the cryostat (1 m distance). For testing components in a cryogenic environment, we chose to use the more readily available and cost effective liquid nitrogen (LN_2) over liquid argon (LAr) [11]. The refractive index of LN_2 is 1.199 at 78 K while the refractive index of LAr is 1.227 at 90 K (see Table 4.1 below) [12]. For testing purposes, the indices are close enough for LN_2 to be workable, and it at least provided a much closer representation to the LAr environment than air or room temperature water.

Material	Refractive Index (*n*) for gas	Refractive Index (*n*) for liquid	Approx US$/cf	Condensation Point (°C)
Helium (He)	1.00003491	*Could not find*	1.3	-268.90
Neon (Ne)	1.00006610	*Could not find*	NA	-246.07
Argon (Ar)	1.00028240	1.2269 (90 K)	0.5	-185.88
Krypton (Kr)	1.00069310	1.3008 (118 K)	NA	-156.60
Nitrogen (N_2)	1.00029839	1.1990 (78 K)	0.2	-195.80

Table 4.1: Refractive index, cost according to 125 cubic feet Airgas cylinder, and condensation/vaporization temperature for noble gases, with the addition of Nitrogen. These values helped us to decide which liquified gas to use for cryogenic testing. *(Ashley)*

The temperature differences between the condensation temperature at standard pressure of argon and nitrogen are relatively small as well, which allowed us to closely model the cryogenic environment of the Far Detector's four cryostats. While any corrections for thermal contraction in LN_2 do not correlate exactly to those in LAr, the conditions closely mirror each other and provided useful insight into problems such exposed components of the camera system may

encounter once employed in the Far Detector. Workability of materials in such an environment was by far our biggest concern and became the main focus of our testing.

4.1 Borescope Cryo-Compatibility *(Ridge, Will)*

To test the viability of a borescope for our applications, we purchased several 7 mm diameter borescopes that are able to be connected to an Android smartphone for testing. Our test here consisted of submitting a borescope to several rounds of thermal cycling to see how it would fair in conditions like those inside the cryostat. First, we connected the borescope to a phone pre-loaded with the CameraFi application, which allows the user to view and take images through externally connected camera devices. Once we were set up to view through our borescope, we submerged the tip of it into liquid nitrogen inside a dewar and recorded how long the camera remained operable. We performed six trials like this with the borescope, and the results are summarized below in Table 4.2.

Trial	Normal Operation	Damaged Picture	Inoperable (End of Test)	Re-Operable after Warmed?
1	3 min	4 min	7 min	Yes
2	2 min	4 min	6 min	Yes
3	1 min	3 min	4 min	Yes
4	0.5 min	1 min	1.5 min	Yes
5	--	--	Immediate	Yes
6	--	--	Immediate	Yes

Table 4.2: Time durations of borescope operability states when submerged in liquid nitrogen, including whether the borescope became operable again when warmed back to room temperature. As an example, in Trial one, the borescope was normally operable for 3 minutes, then sustained a state of damaged picture for 4 minutes, and finally stopped working entirely after 7 minutes had elapsed since the start of the test.

As one may notice, there was a general trend of decreasing operable times as the tests progressed further. Additionally, after every tests, the borescope became normally operable again after it had time to warm back up to room temperature. The “normal operation” state is fairly

self-explanatory; the borescope was able to see clearly and take pictures normally here. In the "damaged picture" state the borescope was still able to take pictures, but the view was pixelated and had flashes of bright color (depicted below in Figure 4.1). When the borescope reached the "inoperable" state, the image either froze or cut to black on the smartphone, and pictures could not be taken anymore. At this point, the trial ended, and we allowed the scope to warm back up. Again, after it warmed following each trial, the borescope returned to normal functionality. Shortly thereafter, we would then begin another trial.

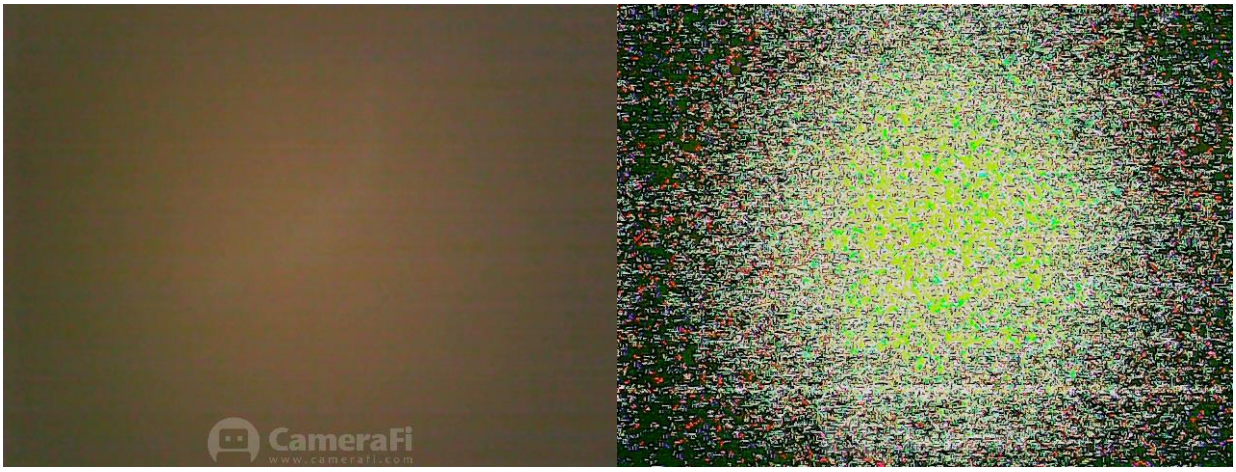

Figure 4.1: Left image, though dark, shows an image through the borescope of the inside of our dewar (Normal Operation). Right image shows the exact same, but with pixilation and flashes of color (Damaged Picture). Both images are from Borescope Test Trial 2.

From the results of our test, it would appear that with repeated thermal cycling, there was lasting damage that affected the borescope's functionality. In each successive trial, it took less time for the borescope to cease functioning entirely, and in the last two trials it became inoperable immediately after placing in the liquid nitrogen. We hypothesized that this loss of functionality came from damage to optical fibers inside the borescope, giving us the observed result. This hypothesis entailed the repeated thermal cycling of the borescope to cause repeated expansion and contraction of the optical fibers, creating enough stress to break them. Reaching the state of inoperability was hypothesized to be because of thermal contraction as well. Wherein the fibers became too warped to relay images effectively.

To investigate this further, we dissected the borescope we used in testing to look for signs of damage. We expected to find broken and fraying fiber optics inside the flexible wire and borescope head but were surprised to find something entirely different. When disassembling the

borescope, we first removed the plastic tip casing. We were able pull it apart rather easily, likely due to damage to the seal caused by submersion in liquid nitrogen. Inside the tip we did find any fibers, but actually found a small solid-state camera (Figure 4.2). We then stripped the black outer layer of the borescope cable and found six color coded copper wires inside (also Figure 4.2). The fact that the anatomy of the borescope was so different than what we expected obviously invalidated our hypotheses about its failure. This also meant that we in fact did not test a fiber optic borescope like we intended. Just because things didn't go as planned though, does not mean this test held no value.

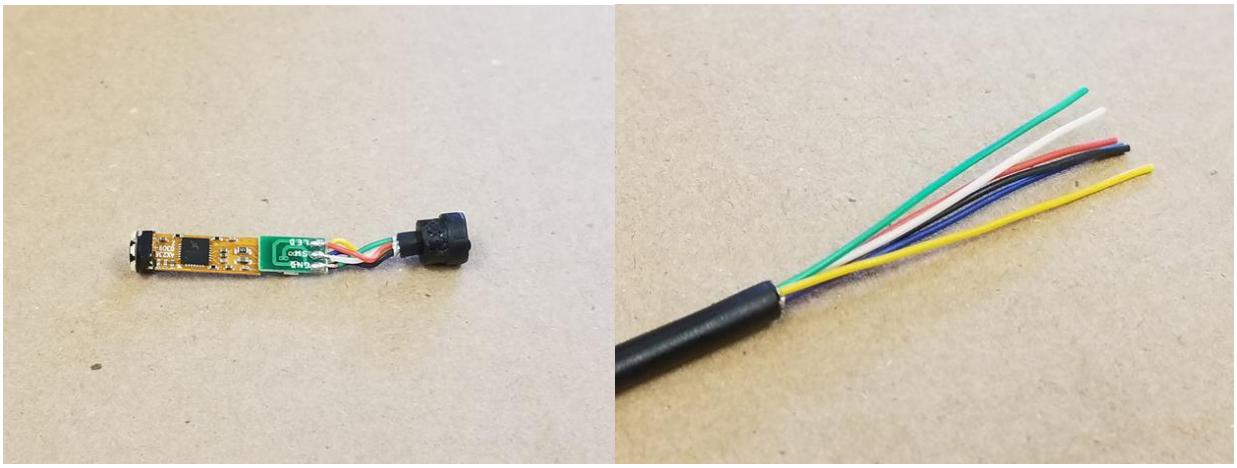

Figure 4.2: Left shows the miniature solid-state camera found inside the tip of the borescope, right shows the color-coded wires found inside the length of the borescope cable.

The failure of the borescope in our liquid nitrogen submersion test here was obviously not due to failure of optical fibers but was more than likely the exact same failure seen in the Raspberry PI cameras used in previous iterations of this camera design. As was discussed previously, in cryogenic conditions, the band gaps inside the semiconductors of electronic components shrink. This shrinkage is of course due to thermal contraction of the material. This test also showed us first-hand the experience of a camera failure of that sort, and as it was our first test protocol using liquid nitrogen, gave us necessary experience working with cryogenic liquid. Primarily due to time constraints and the desire to move on to seemingly more feasible designs, we chose to lay the fiber-optic borescope design to rest and not revisit it.

4.2 Optical Mirror Cryo-Compatibility *(Will)*

In order to test our design option that included mirrors submerged in the cryostat, we first had to build mirrors that would be stable in such an environment. The mirror design that we decided to prototype and build for testing was constructed from a piece of structural fiberglass and a reflective film epoxied to the face of it. The epoxy that we used was a two-part Masterbond product called EP30-2. The datasheet for this product may be found in Appendix A. We chose this particular epoxy because it is optically clear when cured, has a serviceable working temperature range that goes down to 4 K, and is curable at room temperature. The film we used to build our mirrors was a 3M product called Vikuiti Enhanced Specular Reflector (ESR) film. The film is thin, flexible, and reflective on both sides with peelable protective plastic on both sides as well.

To actually construct our mirrors, we cut pieces of both G10 and FRP structural fiberglass to size, as we planned to test whether one offered a favorable design to the other. We also had a few scrap pieces of both types of fiberglass to play with. We then prepared a workstation to coat the fiberglass and apply the ESR film and mixed the EP30-2 epoxy base and hardener. When actually coating mirrors, we experimented with a few different design options, namely: rear-coating the ESR film and attaching to the fiberglass plate (first surface mirror), encapsulating the ESR film and attaching to the fiberglass plate (second surface mirror), and creating one of each of the previous on a piece of G10 and a piece of FRP. We allowed the epoxy to harden for 72 hours and then assessed each mirror. The design that worked best turned out to be the first surface mirrors, with no functional difference between the G10 and FRP plates. The second surface mirrors just turned out to be a sticky mess. An expanded schematic of the chosen mirror design can be found below in Figure 4.3.

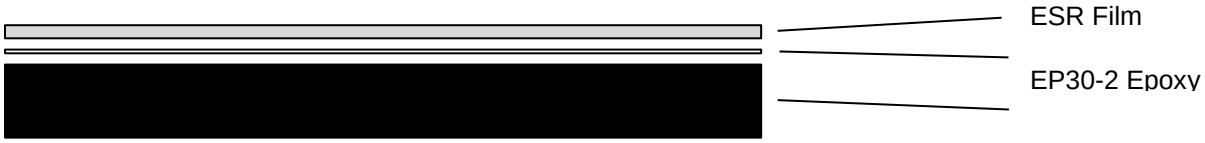

Figure 4.3: Cryogenically compatible mirror with three-layer construction. The size of each constructed test mirror is approximately 4” x 4”.

After construction, we then had to actually test if the mirrors would actually hold up in cryogenic conditions. To do this, we submerged one of the mirrors we made on a piece of an

FRP I-beam in a liquid nitrogen filled dewar (Figure 4.4). The idea here was to subject the mirror to thermal cycling to see if the film would delaminate or unadhere from the fiberglass. To achieve this, we submerged the mirror in four 5-minute increments, allowing it to warm back up to room temperature between trials, and attempted to peel the film off and checked for damage each time. These tests were largely successful, as no damage was sustained even after four rounds of thermal cycling. From this, the mirror implementation aspect of this particular prototype design seems perfectly plausible.

Figure 4.4: Cryo-compatible mirror epoxy system on FRP I-beam. This mirror was tested for functionality through several rounds of thermal cycling. Meter stick is shown for approximate size comparison.

4.3 Lens Cryo-Compatibility *(Ridge, Ashley)*

In addition to testing mirrors for cryogenic compatibility, we needed to test our lenses, as both the mounted mirror and fisheye lens prototype design ideas require lenses to be placed within the cryostat tanks. The lenses that we tested (from Thorlabs) are made of either N-BK7 or N-SF11 optical glass. Three lenses were used here, two controls (uncoated) and one coated with the same Masterbond EP30-2 epoxy that was used above. The two uncoated lenses are Thorlabs' LA1560 (N-BK7) and LD2568 (N-SF11); the coated lens is LA1289 (N-BK7). N-BK7 is the optical material of both lenses (the plano-convex and bi-concave lenses) utilized in our design. The index of refraction for N-BK7 is 1.515, and the index of refraction is 1.785 for N-SF11.

Figure 4.5: Lenses used in LN_2 test. Left and middle are uncoated, right is coated with EP30-2.

The testing of these lenses was rather similar in procedure to the mirror tests. Each lens was submerged into the dewar of liquid nitrogen for five minutes at a time. For this test, we completed four trials all together. After we removed each lens from the dewar, we inspected them for any signs of shrinkage, cracking, or other damage from the thermal cycling. For inspection, we traced their circumferences and performed a "drop test" on each lens to see if they became more brittle and would fracture from a drop height of approximately 1 meter. After four rounds of thermal cycling, the lenses showed no signs of damage, no difference between the cold and room temperature circumferences, and no signs of increased brittleness after submerging them in the LN_2. We made the conclusion that these lenses (both N-BK7 and N-SF11) would work well in the cryogenic environment of the LArTPC, and that coating them in the cryogenically serviceable epoxy was ultimately unnecessary as it would make no difference here. We were also able to show that both optical materials tested would hold up in the cryogenic environment, and we were free to use either in our designs.

4.4 Lens Placement *(Ridge, Ashley)*

As was discussed in section 2.3 Design Requirements, the walls of the cryostat will be roughly 1 meter thick, meaning that any lenses used inside the cryostats will have to be viewed at about a distance of one meter from the camera's sensor. In section 3.2 Optical Design, we were able to provide optical calculations using a system of lenses that would satisfy this requirement. To test the ability to actually attain an image at this distance, we mounted two lenses in lab stands, and placed our Chronos camera one meter from them. As per calculations, we set these lenses about 1 mm and 10 mm apart. The lenses used for our lens placement test were not those used for our lens cryo-compatibility test, as these were the lenses utilized in our prototype design. These lenses (part numbers LA1805 and LD2297) had a 1" diameter. This test was pertinent for both the submerged mirror and fisheye lens designs.

Figure 4.6: The image on the left shows a close-up view through both lenses set on lab stands ~1.5 inches apart. The image on the right shows the screen of the Kron Technologies Chronos 1.4 camera, with a Computar lens set to focus on an object one meter away and zoomed appropriately to achieve the view seen above.

We were able to successfully view through the lens system at a distance of one meter. We adjusted the distance between the lenses and were able to keep a fairly clean image throughout our adjustments. This test gave us the proof of concept needed to move forward with the designs dependent on a lens-camera configuration of this type, and at this distance. It is also important to note that the image seen through both lenses is inverted. It makes no real difference in the design process, but in implementation it is good to know.

4.5 Raspberry Pi *(Will)*

For testing purposes, we chose to work with the Raspberry Pi 3 (Model B) single board computer with the Pi Camera Module V2. We also considered the Pi NoIR Camera V2 in place of the standard V2 camera, but ultimately decided against it, as infrared capabilities were not deemed necessary. Each of these Pi cameras contained a Sony IMX219 8-Megapixel sensor with a frame rate of 60 frames per second (fps). Though this frame rate was much lower than what was needed, the idea was to use this system to test the functionality of our optical designs. Unlike the previous camera systems used, none of our electronics were within the cryogenic liquid itself, so we were optimistic that there would be a higher chance of success in keeping our system up and running.

The Raspberry Pi 3 was implemented in two ways. It was first programmed to simply start and stop recording video on the Chronos 1.4 camera. Second, it was used to rotate a DC motor left and right. This was all done using the coding language, Python, in an application called Idle.

The coding that went into controlling the starting and stopping of video by the Raspberry Pi was really quite simple. Three lines of code sum up this entire process:

```
camera.start_recording('video.Chronos1')
sleep(5)
camera.stop_recording()
```

The start_recording and stop_recording commands are self-explanatory. Meanwhile, the sleep command is there to tell the camera how long to record for (in seconds). In this example, the camera is set to record for 5 seconds.

Rotating a DC Motor using the Raspberry Pi required a much more complex methodology. Additional materials required for this operation included a breadboard, jumper cables (to connect everything), an L239D motor driver chip, and 4 AA batteries (with a holder). The first step in setting this up was connecting the power and ground wires. The common ground used for the entire setup is shown with the black wires:

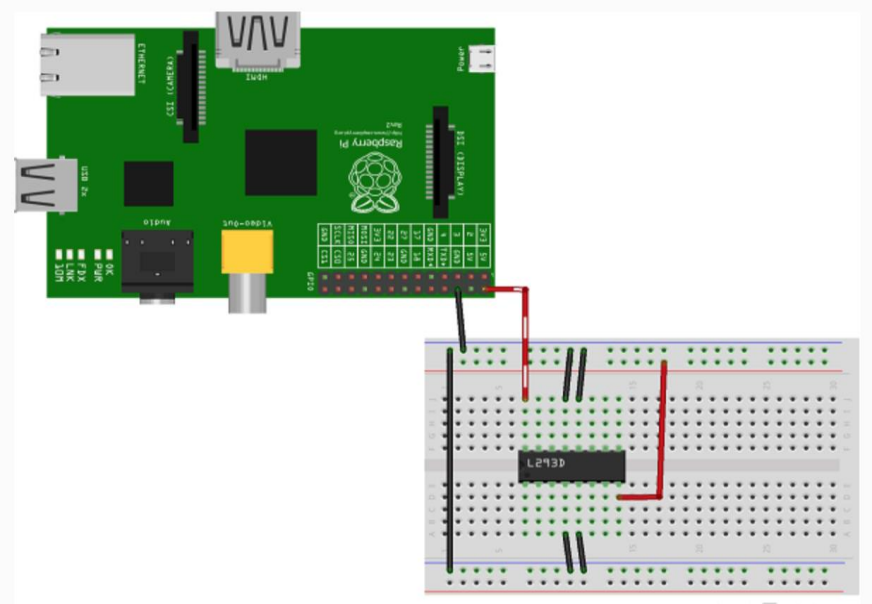

Figure 4.7: Raspberry Pi connected to breadboard via power and ground wires

After adding three wires from the GPIO pins to the L293D, the motor (attached with two wires), and the 4 batteries, the design looked something like this:

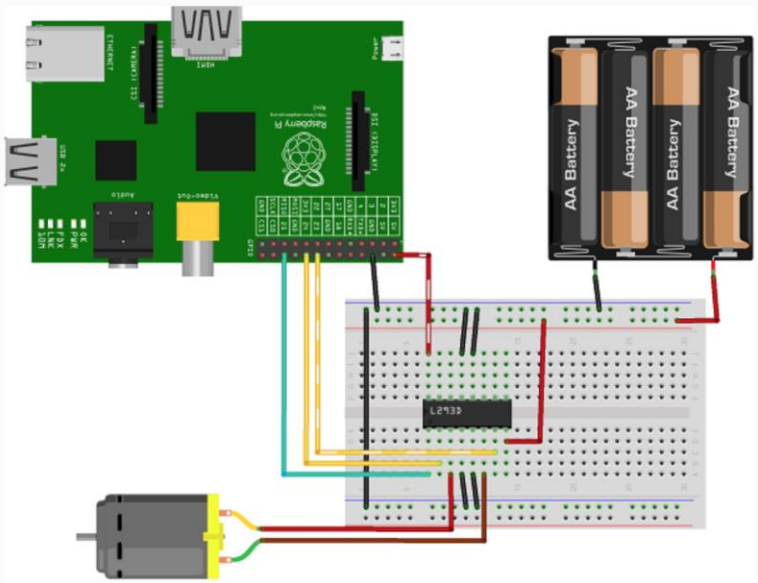

Figure 4.8: Final apparatus with attached DC Motor and Raspberry Pi

Finally, a code was written to be implemented in the Raspberry Pi and control the DC Motor. The following code was created to have the DC Motor rotate right and left before coming to a halt.

```
import RPi.GPIO as GPIO
from time import sleep

GPIO.setmode(GPIO.BOARD)
Motor1A = 16
Motor1B = 18
Motor1E = 22
GPIO.setup(Motor1A,GPIO.OUT)
GPIO.setup(Motor1B,GPIO.OUT)
GPIO.setup(Motor1E,GPIO.OUT)
print "Going forwards"
GPIO.output(Motor1A,GPIO.HIGH)
GPIO.output(Motor1B,GPIO.LOW)
GPIO.output(Motor1E,GPIO.HIGH)
sleep(5)
print "Going backwards"
GPIO.output(Motor1A,GPIO.LOW)
GPIO.output(Motor1B,GPIO.HIGH)
GPIO.output(Motor1E,GPIO.HIGH)
sleep(5)
print "Now stop"
GPIO.output(Motor1E,GPIO.LOW)
GPIO.cleanup()
```

This code, while involving more commands, was still fairly simple. Starting from the top, Motors 1A, 1B, and 1E, each stand for different things. Motors 1A and 1B represent the single motor rotating right and left, respectively. Motor 1E serves as the ‘Master switch,’ as nothing

will run if this is not set to “HIGH.” (The ‘E’ in Motor 1E stands for “Enable.”) Next, where each motor is given an integer (16, 18, and 22), these designations were used to tell Python which pins were associated with the motors. “HIGH” and “LOW” in this case mean on and off, respectively. And the sleep command had the same purpose as previously shown; it serves as the time limit for the motor to run. The following is a truth table that perfectly explains how the apparatus runs with each motor setting:

Enable	A	B	Result
Low	High	Low	Not spinning - Enable is off
Low	Low	High	Not spinning - Enable is off
High	Low	Low	Not spinning - Both inputs are off
High	High	Low	Turning clockwise*
High	Low	High	Turning counter-clockwise*
High	High	High	Not spinning - Both inputs are on

* Direction is down to the motor

Table 4.3: Truth table explaining what each motor setting (High/Low) means for how the apparatus will run (Turning clockwise, counter-clockwise, or not at all).

Chapter 5

Prototyping and Construction

5.1 Prototype Approach *(Ridge, Will)*

The design that we chose to implement and ultimately prototype was the fisheye lens system. We chose this for the simplicity of its design, its relative ease of manufacturing, and the fact that it met all of the necessary design requirements. For the prototype, we needed a rigid tube to mount our design components, optical elements, a mount to hold it inside the tube, a mount to hold the tube itself to the exterior of the cryostat, as well as a way to mount an actual camera to the tube. The structural material used for our design was aluminum, due to a combination of its strength, corrosion resistance, availability, and its non-magnetic material properties (important in considering the final product as the TPC elements/wire planes of the far detector produce a high voltage electric field).

The tubing was custom made, as were the various mounts and flanges needed. We decided to have the lenses purchased through an online lens manufacturer instead of machining them ourselves. We looked into several companies offering custom lenses that would meet our specifications, such as Galvoptics, Custom Scientific, and Meller Optics. Due to time limitations, we opted to go with premade lenses for prototyping; with our top choice companies being Edmund Optics and Thorlabs. We ultimately decided on Thorlabs due to the larger variety of not only size and focal lengths, but also lens material. There was also more readily available data provided for each lens available.

5.2 Camera Interfacing *(Ridge)*

For our design, we implemented the Chronos 1.4 camera from Kron Technologies. Kron Technologies is a crowd-funded company that started on Kickstarter. Their camera offers professional imaging with full customizability of frame rate and resolution, as well as many other features. The Chronos has a maximum resolution of 1280 x 1024 at 1,057 fps and a maximum frame rate of 21,649 fps at a resolution of 640 x 96. The data sheet for the camera may be found in Appendix B of this document for more information.

The frame rate needed to properly capture the visual effects of neutrino interactions in the LArTPC is approximately 1,200 FPS [13]. The 1,502 FPS setting on the camera will provide the necessary frame rate and give an output of 720p video, which will be a reasonable resolution for our applications. A remote controlling software package will eventually be available for download from the camera's developer, but this is noted to be at a later time. If need be, we will compensate with another program. Our main concern for prototyping is image collection; automation will come later.

Recording Rates

Resolution	FPS
1280 x 1024	1,057
1280 x 720	1,502
1280 x 512	2,111
1280 x 360	2,999
1280 x 240	4,489
1280 x 120	8,923
1280 x 96	11,119
1024 x 768	1,771
1024 x 576	2,359
800 x 600	2,873
800 x 480	3,587
640 x 480	4,436
640 x 360	5,903
640 x 240	8,816
640 x 120	17,424
640 x 96	21,649

Table 5.1: This table compares common resolution settings to the corresponding frame rate for the Chronos 1.4 Camera. The resolutions above are only those commonly used, a resolution of any pixel size is possible within the camera's UI. It should be made clear though that increasing frame rate comes at the cost of drastic reduction in resolution.

Figure 5.1: The Chronos 1.4. The camera body and lens are sold separately and we intend on purchasing both, as we may need the lens for testing purposes and possibly for implementation as optical focus in the final design.

Kron Technologies sells the Chronos camera, as well as various accessories to go with it. When we ordered our camera, we also ordered a Computar 12.5-75mm f/1.2 Zoom lens. The lens and camera body can be found pictured above in Figure 5.4. For our one-half scale prototype, we plan to mount the Computar lens with the camera body attached to it. For the full-scale model, we plan to construct a mount that will directly screw into the face of the camera body.

At this time, the operating system of the Chronos is still in the beta stage of production, so several functions supported in hardware are not yet supported in software. These include, but are not limited to HDMI, ethernet, and audio connection and functionality. At this time, it is unclear when these features and others will become available. More information on this is also available in the camera's data sheet.

5.3 Prototype Construction *(Ridge)*

Following our design approach decision and calculations, we were finally able to construct a prototype. For the sake of simplicity in the prototyping process we decided to construct a one-half scale prototype. We would design for the full-scale model, moving on to that if time allowed. The body of the one-half and full-scale models are both one meter long solid cast aluminum tubes; the diameter of the one-half scale is three inches, and the full scale is six inches.

For our three-inch prototype, the design is essentially the same as the schematic seen in the optical design Section 3.2. There is a mount for the camera on the top, with optical lenses and a lens mount at the base. The aluminum body houses all other components of the design, with the camera mount affixed to the top via four screws. There are corresponding screw holes drilled into the aluminum body for these. At the opposite end, which is the end that would be placed in cryogenic liquid, there is a mount for the lens assembly. These are found at either end of the exploded view of the assembly below (Figure 5.2: Right). Both the camera lens and optical lens assembly mounts were 3D printed for use in the prototype, they were modelled and pictured in white to illustrate this. For the purposes of modelling, since we were unable to test our prototype in LN_2, the use of plastic components was sufficient here.

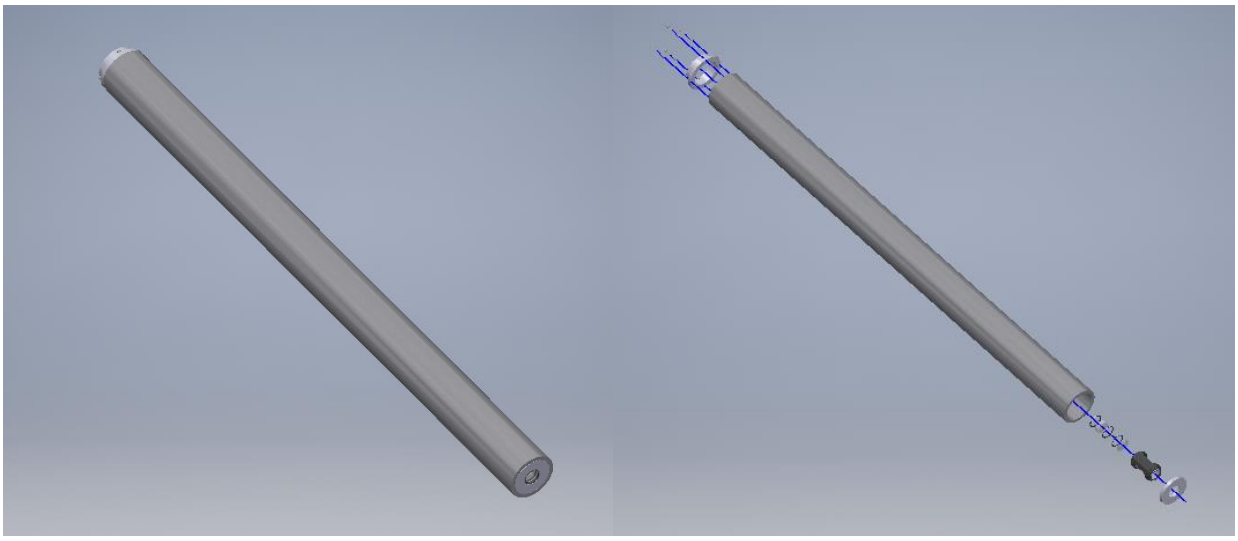

Figure 5.2: The 3-inch prototype assembly (left) and exploded view (right) are shown here. In the exploded view, parts were moved linearly from their true locations along the blue lines. The lens assembly (bottom right of exploded view) is shown in greater detail later in this section. Detailed and annotated drawings of all components created using CAD software here and throughout may be found in Appendix C. *(Ridge)*

This prototype model is designed to mount the Chronos' lens directly to it, and thus allow for imaging that way. The lens is mounted to the top by snuggly sliding into the mount and held in place using set screws that line up and fit with the set screw holes already in the lens body. The lens assembly mount holds the lens assembly tube by snapping into the hole in the center, and the mount itself fits into the prototype body by sliding firmly into place at the end of the tube. In a more permanent design configuration, or at least one that would be tested in a cryogenic environment, these components would likely be secured using set screws or a cryogenically serviceable epoxy like the Masterbond system used in the Testing and Development chapter.

The working optical components of the prototype, mounted at the base of the body, are housed in a lens tube that was purchased from Thorlabs along with the lenses themselves. The lens tube is two inches in length and hold one inch diameter lenses. The interior of the tube is threaded, allowing retaining rings that are also available for purchase from Thorlabs to be screwed into the tube. These rings hold the lenses in place and can of course be adjusted for focusing and alignment purposes. The tube itself, designated as SM1L20C in Thorlabs' catalog, also has an outer sleeve that can be rotated to close the gaps in the side that can be seen below in the assembly (Figure 5.3). Closing the gap is useful for making the tube light tight, but for our purposes where the body of the prototype is already light tight by design, the function of the outer sleeve is vestigial. As discussed previously, the two lenses used in our optical assembly are Thorlabs' LA1805 plano-convex (front) and LD2297 bi-concave (back), with focal lengths of 30 mm and -25 mm respectively. Inside the tube, the lenses are approximately 10 mm apart.

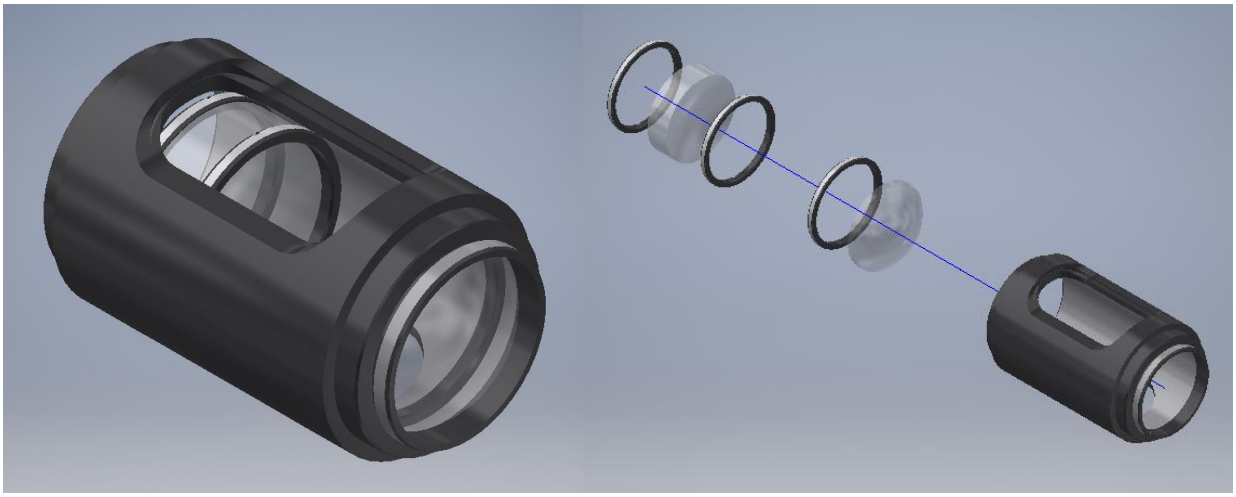

Figure 5.3: The lens assembly and exploded view are shown here. They contain the slotted lens tube (SM1L20C), wherein the plano-convex (LA1805) and bi-concave lenses are mounted using retaining rings (SM1LTRR). *(Ridge)*

In practice, the assembly and use of the lens tube is rather simple; one simply needs to screw the retaining rings up and down to adjust lens focus and construct an optical system. In our case, with our lens assembly, it is also worth noting that the image seen through the lenses is inverted. This is visible, though not terribly obvious is Figure 4.6 of the previous chapter. The test in which the two lenses were used served a double function in this way.

Overall, we were met with success with our one-half scale prototype. As a proof of concept, things could not have gone much better. The design allowed us a 180° field of view, and we were able to view successfully through our camera to capture an image at a distance of one meter.

However, this edition of the prototype lacks certain key features that would be necessary for the final design. Namely, the obvious fact that the diameter is half of what it should be; it also lacks a way to mount the final constructed system to the cryostat; the optical lens assembly is held together essentially by friction, and has plastic components, neither of which are necessarily favorable in a cryogenic liquid environment, and this system mounts our camera's lens, rather than the camera body itself.

From here, we were able to move on to the full-scale prototype. This model will have a body diameter of six inches, as that is the diameter of the viewports in the top of the cryostat. After cutting a tube for the body, we designed a mount for the camera at the top of the cryostat. This mount, as opposed to the three-inch prototype mount, directly screw into the camera body. The screw mount uses the generic camera C-mount lens thread pattern 1-32 UN-2A. This thread designation stands for a one-inch diameter screw with 32 threads per inch of length. The six-inch mount is affixed to the tube body just as the previous one was, with four screws holding it in place. The most notable difference here though, is the four large plates extruding from the mount's main body. Each of these plates have a hole drilled through them, and the holes are threaded to accept a standard one-half inch hex bolt. These are designed to be able to mount the entire assembly to the exterior of the DUNE cryostats. These design features can be seen in detail below in Figure 5.4, and in even greater detail in Appendix C. As with the three-inch prototype, we had the mount shown below 3D printed; the printed part is again shown in white to illustrate this fact.

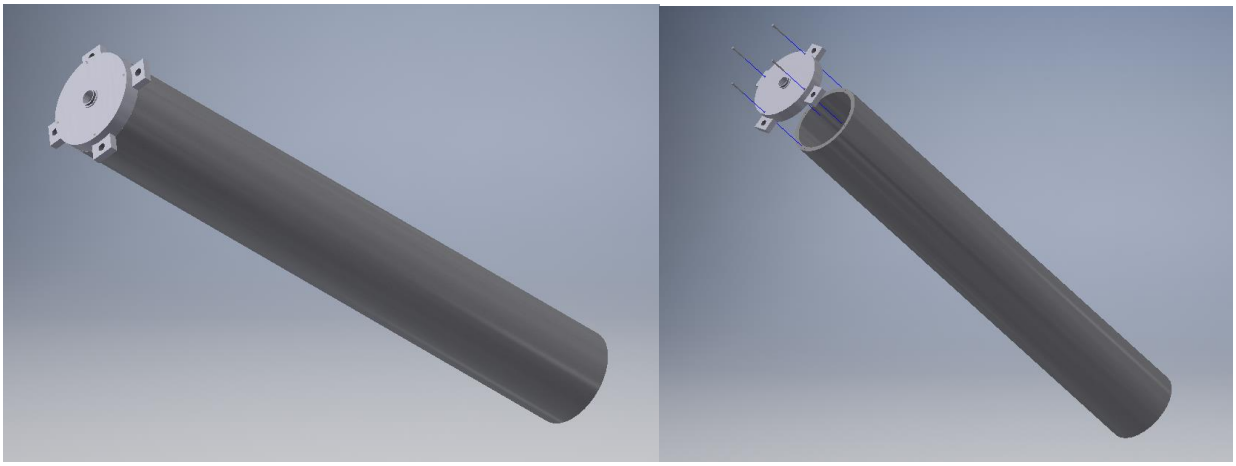

Figure 5.4: These are the 6-inch prototype assembled and exploded views. The only major design components here are the prototype's body and the mount affixed to the top of it. For this reason,

and to show better detail, the isometric view of these assemblies has been rotated 90° from the point of view of the others shown in this chapter. *(Ridge)*

Due to time limitations, we were unable to move further on the prototype design for the full-scale model. In the full-scale model, the lenses would be bigger (55 mm in diameter, as mentioned in Optical Design section), meaning a new custom lens assembly would need to be constructed alongside the custom lenses. Along with this, both the lens assembly and lens assembly mount will have to be cryogenically compatible--meaning no more plastic parts. This goes for the camera mount at the top of the body too, to realistically model conditions for the final system in place in the DUNE cryostats, all parts would likely be machined from aluminum. In the optical design for this system, without the use of the camera lens capable of zooming in on an image, it would also be necessary to have a way to enlarge the image inside the tube for viewing with the camera's sensor. To achieve this, perhaps another array of lenses would be needed closer to the top of the body.

In addition to the physical components of the design, many of the software-based components of the design could not be implemented due to time limitations. As discussed in Section 2.3, there were design requirements that included the sparsifying of data collected, as well as remote controlling digital zoom capabilities and the operation of the system itself. In future software releases, Kron Technologies intends to offer a free package to users that includes the ability to control many of the functions of their Chronos 1.4 remotely. It is unclear when such a release will occur, and what the exact nature and capabilities of this future software will be at this time. It is also unclear if such a software package will satisfy the needs of this project in terms of remote operation. One feature that will definitely meet the needs of the project in the future though, is real-time streaming. Future software releases will also include the functionality of certain camera components currently supported in hardware, but not software (as mention in Section 5.2). This includes features like HDMI and ethernet connection capability, which will be able to be used to stream video from the Chronos in real time. Elementary remote operation capabilities were intended to be implemented using a Raspberry PI board, but again, we did not have enough time to design for this.

Chapter 6

Conclusions, Results, and Reflection

6.1 Project Timeline *(Will, Ridge)*

During the Fall 2017 semester, we made administrative progress in laying the groundwork for our project and took / the first steps into the engineering design process. During the month of September, we met with Dr. Nelson the first few times, discussed what type of project this was to be, and what it would entail. In October, we began doing background research and compiled a list of criteria and constraints for our design. November was our brainstorming month, when we came up with a list of possible solutions and worked together to narrow them down to the most viable options (these were discussed in Section 3.1). Finally, December was designated primarily for work with our thesis and Midterm presentation, with a few other small tasks thrown in.

As a tool for both planning and the distribution of tasks during the Spring 2018 semester, we used Gantt charts to create a visual representation of the steps we took throughout our project. This was an organizational step up from our relatively unorganized first semester. Below are two snapshots of Gantt charts used to plan tasks for the Spring 2018 semester. The first Gantt chart was completed in preparation for the Midterm presentation last semester as a plan for the future (Figure 6.1); the second was completed during the month of April in retrospect of how long each task actually took to finish. The far-left sides of the charts begin in the month of December 2017, and the far right concludes in April 2018. The length of the green bars in the charts are indicative of the time needed to complete the associated task. The time scale is located at the top in gray, and each bar's task is listed at the right end of it, after the completion date. For the sake of simplicity, the tasks in both charts are listed in the same order with the same names, though there are some minor additions/alterations.

Figure 6.1: This is the Gantt Chart as of December 2017. This was intended as a plan of operations for the Spring 2018 semester; note the tasks here are relatively clean-cut and sequential. Also note that not many tasks overlap, and there are clear times allotted for each one.

Figure 6.2: This is the Gantt Chart as of April 2018. This version shows how long tasks actually took to complete looking back. Note here that nearly every single task took longer to complete than was expected in Figure 6.1. There is also a significant amount of overlapping of tasks, which led to the bunching up of tasks toward the end of the project.

From the figures, it is clear that our initial plans for how the project would play out were not met. It took longer than expected to complete nearly every task we set out to do; and as it was mentioned in Section 5.3, several aspects of our design that we wanted to complete were left out due to a lack of time. For the most part, it is safe to say that our time struggles were due mostly to a lack of organization. We were able to get quite a bit done, but with slightly more structure and oversight in the project, we likely could have made it a lot farther. In the last month of the project, many tasks were rushed and we had quite a few things going on at once; this is evident in the Gantt chart in Figure 6.2. The rush in the final weeks left an undesirably short amount of time for administrative tasks and completing the writing requirement. Better structure of the project and better time management could have made for a greater result all around.

6.2 Project Budget *(Will)*

Over the course of this project, various materials were ordered for use in the testing and prototyping phases of our design. There were several smaller orders of parts for testing, safety equipment, and various odds and ends. The largest order that consumed nearly half of the budget though, was the Chronos 1.4 camera from Kron Technologies; this order consumed a whopping $3,511.20. The second largest allocation of funds then came from the testing for the mirror system design option. The Master Bond epoxy systems used costed a total of $1,950.00, the 3M Vikuiti ESR film used to create the cryogenic mirrors costed $700.49, and the structural fiberglass that we purchased costed $118.99. Those three items together total nearly $3,000. In addition to better time management like was mentioned in the previous section, our team could have used a little better financial planning. The camera was certainly a good investment, but all of the materials purchased for a design we did not implement was definitely not.

Other materials were attained through the generosity of the Machine Shop and Makerspace teams in the William and Mary physics department, and are not listed in the budget Table 6.3 below. These items included the aluminum tubing used for both the one-half scale prototype and full scale models in our design, as well as various parts we had 3D printed to construct our prototypes.

Date	Merchant	Item	Item Price	Total
1/26/2018	Amazon.com	1.5M Endoscope	$7.36	$7.36
		Shipping & Tax	$0.00	
1/26/2018	Amazon.com	Raspberry Pi Camera Module v2	$28.99	$65.93
		Raspberry Pi Model B Motherboard	$36.94	
		Shipping & Tax	$0.00	
1/26/2018	Kron Technologies	Chronos 1.4 High Speed Camera w/ Computar lens	$3,378.00	$3,511.20
		Trigger Switch	$35.00	
		Shipping & Tax	$98.20	
2/5/2018	Master Bond, Inc.	EP29LPSP Epoxy	$975.00	$1,950.00
		EP30-2 Epoxy	$975.00	
		Shipping & Tax	$0.00	
2/8/2018	Amazon.com	6ft HDMI Cable	$6.99	$477.18
		6ft eSATA Cable	$6.89	
		ZoMei Z818 Heavy Duty Tripod	$104.99	
		3M Ratchet Headgear H8A	$19.03 x5	
		3M Replacement Faceshield WP96	$7.04 x5	
		Inf-way 38cm Cryo-Gloves	$56.99 x4	
		Shipping & Tax	$0.00	
3/19/2018	Amazon.com	5.0M Endoscope	$13.99 x5	$69.95
		Shipping & Tax	$0.00	
3/27/2018	Thorlabs	LA1289 Plano-Convex 1/2"	$19.38	$153.39
		LA1560 Plano-Convex 1/2"	$19.69	
		LA1951 Plano-Convex 1"	$23.70	
		LA1805 Plano-Convex 1"	$23.20	
		LD2568 Bi-Concave 9mm	$26.27	
		LD2297 Bi-Concave 25.4mm	$33.15	
		Shipping & Tax	$8.00	
3/28/2018	McMaster-Carr	24"x24"x3/8" Structural Fiberglass	$107.72	$118.99
		Shipping & Tax	$11.27	
3/30/2018	Digi-Key	30 PCS 3M Vikuiti ESR Film	$688.50	$700.49
		Shipping & Tax	$11.99	
4/9/2018	Thorlabs	LA1805 Plano-Convex 1"	$23.20	$138.36
		SM1L20C SM1 Slotted Lens Tube 2"	$62.48	
		SM1LTRR SM1 Retaining Ring	$22.34 x2	
		Shipping & Tax	$8.00	
			Grand Total:	$7,192.85

Table 6.3: This table shows all items purchased for use in our project, where they were purchased from, as well as unit prices and order totals. The total spent over the course of the project reached just shy of $7,200.

6.3 Conclusions and Future Plans *(Ashley)*

Over the past year, our research team worked on engineering a camera system to be used within the four LArTPCs of the Far Detector, an integral part of the Deep Underground Neutrino Experiment. We worked on three different prototype ideas before concluding a final design which would employ a high quality, scientific camera and utilize a system of lenses. We decided on using the Kron Technologies Chronos camera for our final design and a Raspberry Pi 3 Model B for use with our prototype, though we did end up implementing the Chronos camera into both designs. For prototyping, we constructed a one-half scale model of what the final design to be used for the DUNE would be. This prototype was built on our most successful design idea from a series of laboratory test. These tests mainly consisted of the ability of submerged design components to withstand supercooled temperatures and thermal cycling, as well as the compatibility of each design with our camera, which would be positioned outside of the cryostat. Our objective in these tests was to work out which would be the more feasible option in terms of ease of construction and implementation with our camera.

These three design ideas (the fisheye lens system, the mirrored cryostat, and the fiber-optic borescope) had varying degrees of success. The first, our fisheye lens system, required us to work through simple optical calculations before we were able to begin testing. The optics led us to conclude that a system of lenses would be the appropriate approach in construction of this prototype. After consideration on having custom lenses produced or to simply alter our calculations and have these lenses purchased for our prototype, we decided on ordering a 30 mm plano-convex (converging) lens and a -25 mm bi-concave (diverging) lens from Thorlabs. Several other lenses of the same material (N-BK7 optical glass) were purchased and used to test for cryo-compatibility of this material. Our test shown them to withstand thermal cycling and so we concluded that they would not need to be protected from the interior of the cryostats. This design was the preferred arrangement and is the design in which our prototype was built on.

Our second idea, the mirrored cryostat, called for either a system of mirrors to be placed throughout the chamber, or to simply have one large mirror placed at the base for the camera to be focused on. Before testing for cryo-compatibility, we needed to create a mirror that we believed would plausibly work in this environment. For this design, we constructed our mirror out of a fiberglass base which was glazed with an epoxy (EP30-2) before being coated with an

enhanced specular reflector (ESR) film. Liquid nitrogen submergent testing proved this to be a feasible option in terms of being put into effective operation.

Our third idea, the borescope design, did not make it past testing. We bought a number of HD, Android Camera borescopes in hopes to experimenting with the functionality of quartz fiber optics in a cryogenic environment (as this is something we found to be not widely known). The image did not withstand thermal cycling, and once the failed borescope was dissected, we found that the cable consisted of coated copper wires, not the bundle of quartz fibers we had imagined. The solid-state camera of the borescope was positioned at the end of the device (which had been submerged), not towards the connector as we initially believed. We concluded that the failure of the borescope was the same failure as seen in the Raspberry PI cameras used in previous designs for the DUNE camera system.

Though we did not finish constructing a final model for our system, we did complete the design layout along with physical work on several elements, including having the pipe machined and having all optical components from the prototype adaptable for use in this model. In the future, we would like to construct completed aluminum mounts for components and to have our full-scale model tested for functionality with the Chronos camera. The lens system we purchased turned out to be a great match for prototype and final design alike, though custom machined lenses would be an option if lens size is a concern for the actual camera system to be employed in the detectors as they are completed and begin work.

Appendix A

Masterbond EP30-2 Technical Datasheet

EP30-2 Master Bond Polymer System

Two component, room temperature curing epoxy system for bonding, sealing, coating and encapsulation featuring a wide range of desirable properties

Key Features

- ✓ Extremely optically clear
- ✓ Superb physical strength properties
- ✓ Meets NASA low outgassing specifications
- ✓ Cryogenic serviceability
- ✓ Outstanding electrical properties
- ✓ Withstands 1,000 hours 85°C/85% RH

Product Description

Master Bond EP30-2 is a lower viscosity, two component epoxy system combining a number of highly desirable attributes. It is easily processed and has a non-critical ten to one mix ratio by weight. EP30-2 cures readily in 24-48 hours at room temperature or more rapidly at elevated temperatures, e.g. 2-3 hours at 150-200°F. The optimum cure is overnight at room temperature followed by 2-3 hours at 150-200°F. This epoxy flows smoothly and evenly after mixing, and is easily applied as an adhesive, coating or potting material.

EP30-2 has great optical clarity. Its physical strength profile, especially tensile, tensile lap shear and compressive strength, among others is most impressive. It is a terrific electrical insulator and is well suited for smaller potting and encapsulation applications. It is a highly structural system, that is to say it is rigid without being brittle. It is very dimensionally stable with low shrinkage upon curing.

EP30-2 is a superior adhesive that bonds well to a wide variety of substrates including metals, composites, glass, ceramics and many rubbers and plastics. EP30-2 is highly resistant to water, oils, fuels, acids, bases and many solvents. EP30-2 also has been used successfully in a number of cryogenic applications. Its service temperature range is from 4K to +300°F. It passes NASA low outgassing specifications. This exceptionally versatile system can be used in a variety of applications in aerospace, electronic, optical and specialty OEM industries, especially when optical clarity and low outgassing are important criteria.

Product Advantages

- Convenient handling and processing
- Favorable physical strength profile
- Compelling optical clarity and light transmission
- Very low shrinkage upon curing
- A "go-to" material for small potting and encapsulation applications

Typical Properties

Tensile lap shear strength, aluminum to aluminum, 75°F	3,000-3,200 psi
Tensile strength, 75°F	10,000-11,000 psi
Compressive strength, 75°F	14,000-15,000 psi
Hardness, 75°F	80-90 Shore D
Hardness after 1,000 hours 85°C/85% RH	90 Shore D
Coefficient of thermal expansion, 75°F	40-45 x 10^{-6} in/in/°C
Dielectric strength, 75°F	440 volts/mil
Volume resistivity, 75°F	>10^{15} ohm-cm
Dielectric constant, 75°F, 60Hz	3.5
Refractive index, 75°F	1.55
Service temperature range	4K to +300°F [4K to +149°C]

Mixing and Curing

Mixing ratio, Parts A to B	10:1 by weight
Viscosity, Part A, 75°F	10,000-16,000 cps
Viscosity, Part B, 75°F	10-35 cps
Working life after mixing, 75°F; 100 gram batch	20-40 minutes
Specific gravity	0.98
Cure schedule options	
75°F	24-48 hours
200°F	2-3 hours
Optimum cure schedule	Overnight at 75°F, followed by 2-3 hours at 150-200°F
Shelf life at 75°F, in original unopened containers	1 year

Preparation of Adhesive

Master Bond EP30-2 is prepared by thoroughly mixing Part A with Part B in a ten to one mix ratio by weight.

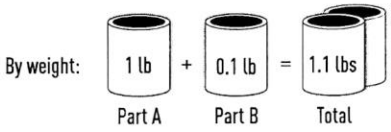

Mixing should be done slowly to avoid entrapping air. The lower viscosity of the two components makes mixing easy. The working life of a mixed 100 gram batch is approximately 20-40 minutes. It can be substantially lengthened by using shallower mixing vessels or mixing smaller size batches.

Preparation of Bonding Surfaces

All bonding surfaces should be carefully cleaned, degreased and dried to obtain maximum bond strength. When bonding to metal surfaces or other substrates, chemical etching or mechanical abrading should be employed so that the bonded joints exhibit optimal properties. In fact, most substrates should be roughened with sandpaper, emery paper or mechanically abraded to maximize adhesion.

Application and Assembly

Master Bond EP30-2 can be conveniently applied with a syringe, brush, paint roller, etc. Enough mixed adhesive should be applied to obtain a final adhesive bond line thickness of 3-5 mils. Porous surfaces may require more adhesive to fill the voids than non-porous ones. Thicker glue lines do not increase the strength of a joint but do not necessarily give lower results as the EP30-2 system does not contain any volatiles. The parts to be bonded should then be pressed together with just enough pressure to maintain intimate contact during cure. Care should be taken not to squeeze out the adhesive during fixturing. In casting and potting applications, it may be necessary to vacuum degas in order to remove the relatively few air bubbles that may have been formed when mixing.

Cure

Master Bond EP30-2 can be cured at room temperature or at elevated temperatures as desired. At room temperature, EP30-2 cures within 24-48 hours. Faster cures can be realized at elevated temperatures, e.g. 2-3 hours at 200°F. An optimum cure schedule is overnight at room temperature, followed by 2-3 hours at 150-200°F. Remove excess adhesive promptly before it hardens with a spatula. Then wipe with a rag and solvent such as MEK, toluene or acetone. The thinner the section of epoxy, the slower the rate of cure.

Packaging

Product is available in:

- 1/2 Pint kits
- Pint kits
- Quart kits
- Gallon kits
- 5 Gallon kits

Specialty packaging is also available in gun kits.

Handling and Storage

All epoxy resins should be used with good ventilation and skin contact should be avoided. For safe handling details, please consult the product SDS. Optimum storage is at

or below 75°F in closed containers. No special storage conditions are necessary. Containers should, however, be kept closed when not in use to avoid contamination. Cleanup of spills and equipment is readily achieved with aromatic or ketone solvents employing proper precautions of ventilation and flammability.

Certifications

RoHS COMPLIANT

NASA Low Outgassing

Not to Be Used for Specification Purposes

The values contained herein are considered typical properties only and are not intended to be used as specification limits. For assistance in preparing specifications, please contact Master Bond technical support for further details.

Notice

Master Bond believes the information on the data sheets is reliable and accurate as is technical advice provided by the company. Master Bond makes no warranties, expressed or implied, regarding the accuracy of the information, and assumes no liability regarding the handling and use of this product.

Appendix B

Kron Technologies Chronos 1.4 Datasheet

CHRONOS 1.4 DATASHEET Page 1

Chronos 1.4 is a 1.4 gigapixel-per-second handheld high-speed camera. Completely self-contained, you can take high-speed imaging with you anywhere. It records 1280x1024 video at 1057fps, and can record at up to 38 500fps at lower resolution. Video is saved in compressed h.264 or uncompressed RAW format to removable media. You can shoot for hours, saving hundreds of shots on a single card.

Main Features

1.4Gpx/s, 1.3 megapixel image sensor captures 1280x1024 @ 1057fps, and up to 38500fps at lower resolution. Available in color and monochrome. The monochrome option has higher effective resolution and is twice as sensitive as color.

8GB or 16GB memory options for 4 or 8 second record time respectively.

High sensitivity of ISO 320-5 120 (Color), 740-11 840 (Monochrome) enables shooting with modest lighting.

Completely standalone, untethered operation with 1. 5hr internal battery. Runs indefinitely on AC adapter.

"Run-n-Gun" record mode allows you to forget about saving. Take bursts of video by holding the shutter button, and the video is automatically saved to card. You can continue to shoot and view live video while saving, no waiting for the save to complete as long as buffer is available.

Continuous record mode records normal rate video (60fps) continuously to storage devices while simultaneously recording bursts of high-speed video.

Focus peaking highlights sharp edges for quick and perfect focus. Zebra lines help you set correct exposure.

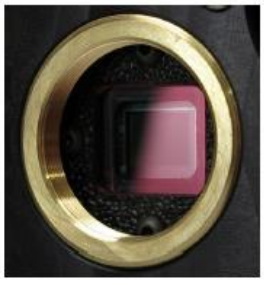

Resolutions and Frame rates

Resolution	Max FPS	Record time (sec) (8GB)	Record time (sec) (16GB)
1280 x 1024	1 057	4.13	8.26
1280 x 720	1 502	4.13	8.27
1280 x 512	2 111	4.14	8.27
1280 x 360	2 999	4.14	8.28
1280 x 240	4 489	4.15	8.30
1280 x 120	8 923	4.17	8.35
1280 x 96	11 119	4.19	8.38
1024 x 768	1 771	4.11	8.22
1024 x 576	2 359	4.11	8.23
800 x 600	2 873	4.15	8.30
800 x 480	3 587	4.15	8.31
640 x 480	4 436	4.20	8.40
640 x 360	5 903	4.21	8.42
640 x 240	8 816	4.23	8.45
640 x 120	17 424	4.28	8.56
640 x 96	21 649	4.30	8.61
336 x 252	15 200	4.43	8.87
336 x 190	20 020	4.47	8.94
336 x 120	31 192	4.53	9.07
336 x 96	38 565	4.60	9.20

Full Specifications

Camera	*Imaging*	1280x1024 1057fps, see resolution table for details
	Memory	8GB or 16GB
	Record time	4 seconds (8GB), 8 seconds (16GB)
	Lens mount	CS mount, C mount with included adapter
	Backfocus	Field adjustable
	IR Filter	650nm, user removable, 18 x 18 x 1.1mm
	Display	5" 800x480 capacitive touchscreen
	Enclosure	Anodized CNC machined aluminum
	Cooling	Active cooling, variable-speed fan
	Dimensions	155mm x 96mm x 67.3mm (6.11" x 3.78" x 2.65") without lens
	Weight	1.06kg (2.34 lbs) without lens
Video formats	*H.264*	Industry-standard mp4 files at bitrates up to 60Mbps
	*cinemaDNG Raw**	Standard Adobe cinemaDNG raw files

Continued ›

Image Sensor	*Resolution*	1280x1024 @ 1057fps
	Speed	1.4Gpx/s - Full throughput down to 336 pixel image width
	Dimensions	8.45 x 6.76mm
	Pixel pitch	6.6um
	Sensitivity (ISO)	Color - ISO 320 to 5 120 Mono - ISO 740 to 11 840
	Shutter	Electronic global shutter, 1/fps to 2us (1/500 000 s)
	Dynamic range	56.7 dB
	Bit depth	12-bit
Battery	*Type*	EN-EL4a
	Runtime	1.5 hours recording
	Charge time	2 hours (0-80%) with in-camera charger
IO	*Power Input*	17-20V 40W 5.5/2.5mm barrel jack, positive tip
	*Network**	Gigabit Ethernet
	Trigger	Two Trigger inputs/frame strobe outputs (BNC and Aux) Adjustable input threshold 0 to 6.6V Electrically isolated trigger input (Aux connector)
	*Audio**	Microphone/Line input, headphone output
	*Video**	HDMI output, video or video+menus
	USB	Two USB host ports (one on mini-B via USB OTG cable)
	SATA	eSATA 3G
	*Analog input**	1MSa/s 12-bit, 200kHz bandwidth, +/- 1V full scale
Trigger modes	*Normal triggered*	Camera records until a defined delay after a trigger
	Triggered start	Camera starts recording a defined delay after a trigger
Trigger Sources	*Electrical*	0-6.6V threshold, optional button debounce and pullup
	*Audio**	Trigger on loud sounds
	*Acceleration**	Trigger on camera motion, tilt or shock
	*Image**	Trigger on image changes
Recording modes	*Normal*	Records into the circular buffer. Once a trigger occurs, video can be reviewed and saved
	*Segmented**	RAM is divided into segments, each recording as in the Normal mode above. Number of segments is user selectable.
	*Continuous**	Video is saved continuously at up to 60fps to mp4 files on removable storage. Operates like a normal video camera.
	*Run-n-Gun**	Bursts of video are saved to RAM while holding down the shutter button. Video is saved to storage devices automatically. More bursts can be captured simultaneously while video is saving.
	*Gated burst**	Frames are captured while trigger is active
	*Normal + continuous**	High-speed video is recorded to the RAM buffer while simultaneously 60fps videos is saved to removable storage

Continued ♪

Shutter timing	*Normal*	Frame rate and exposure time are controlled by camera
	Edge triggered	A single frame is captured on each rising or falling edge of an external input. Exposure is controlled by camera
	Shutter gating	Image sensor shutter is directly controlled by an external input, exposing while the input is active
Assistive	*Focus Peaking*	Highlights sharp edges to aid focusing
	Zebras	Rolling diagonal lines indicate clipped (overexposed) areas
	Focus Aid	Zooms in to allow easier focusing

*These features are fully supported in the camera's hardware, but are not yet supported in software. They will be added in a free software update after the camera's initial release.

Appendix C

Annotated Drawings of CAD Modelled Parts

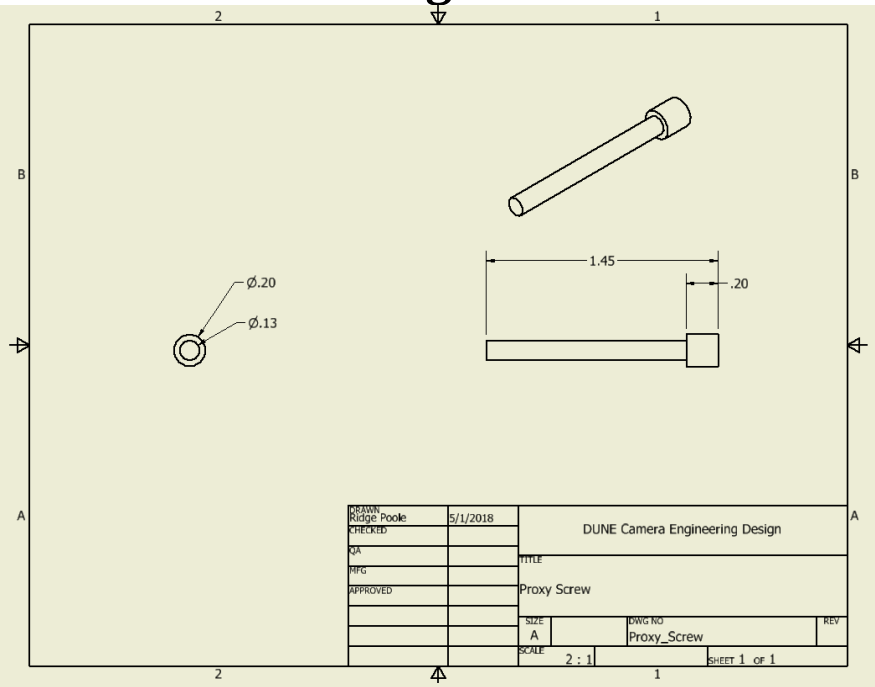

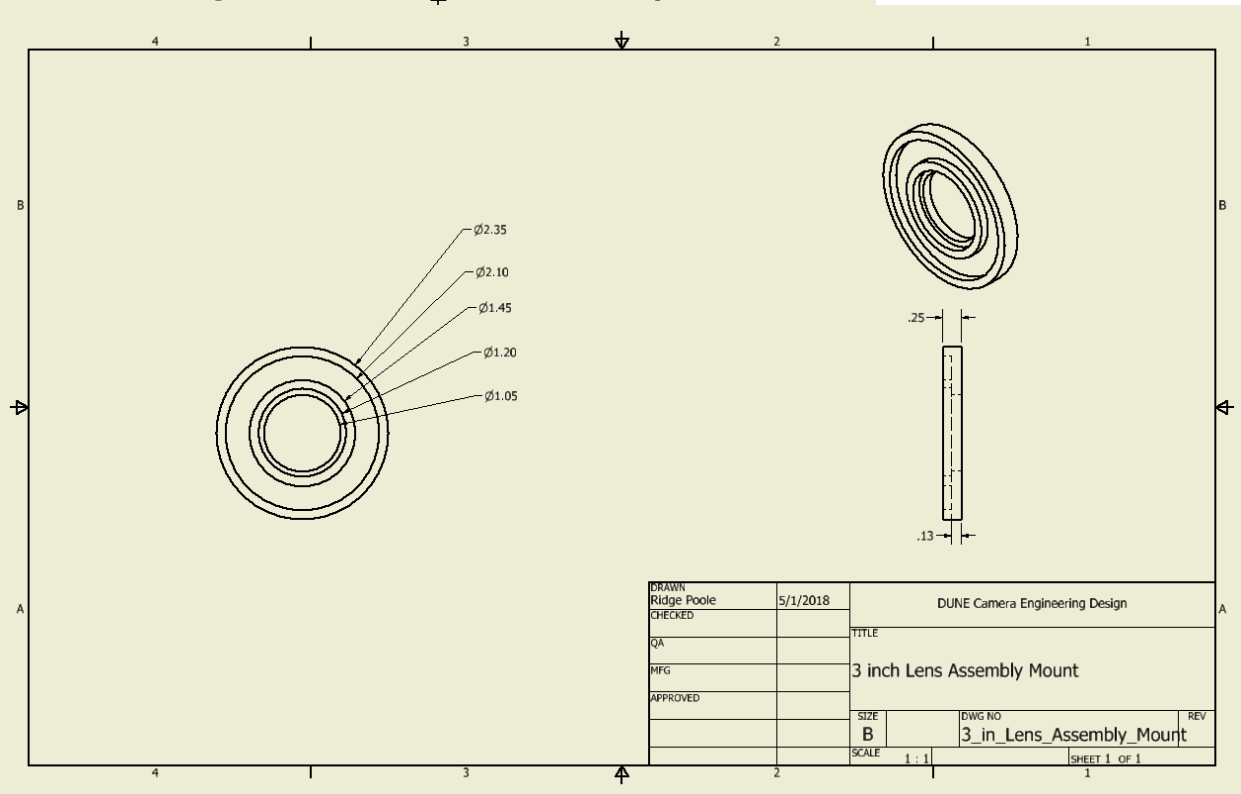

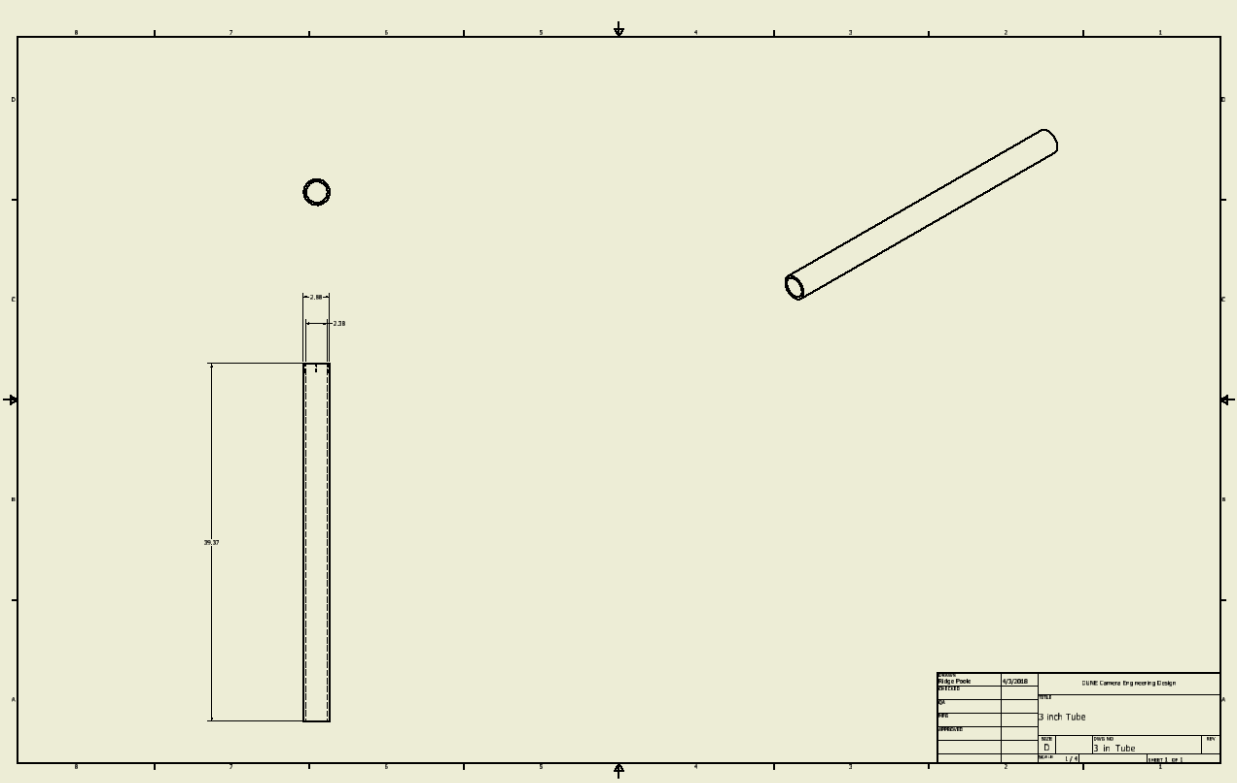
3 inch Tube
3 in Tube

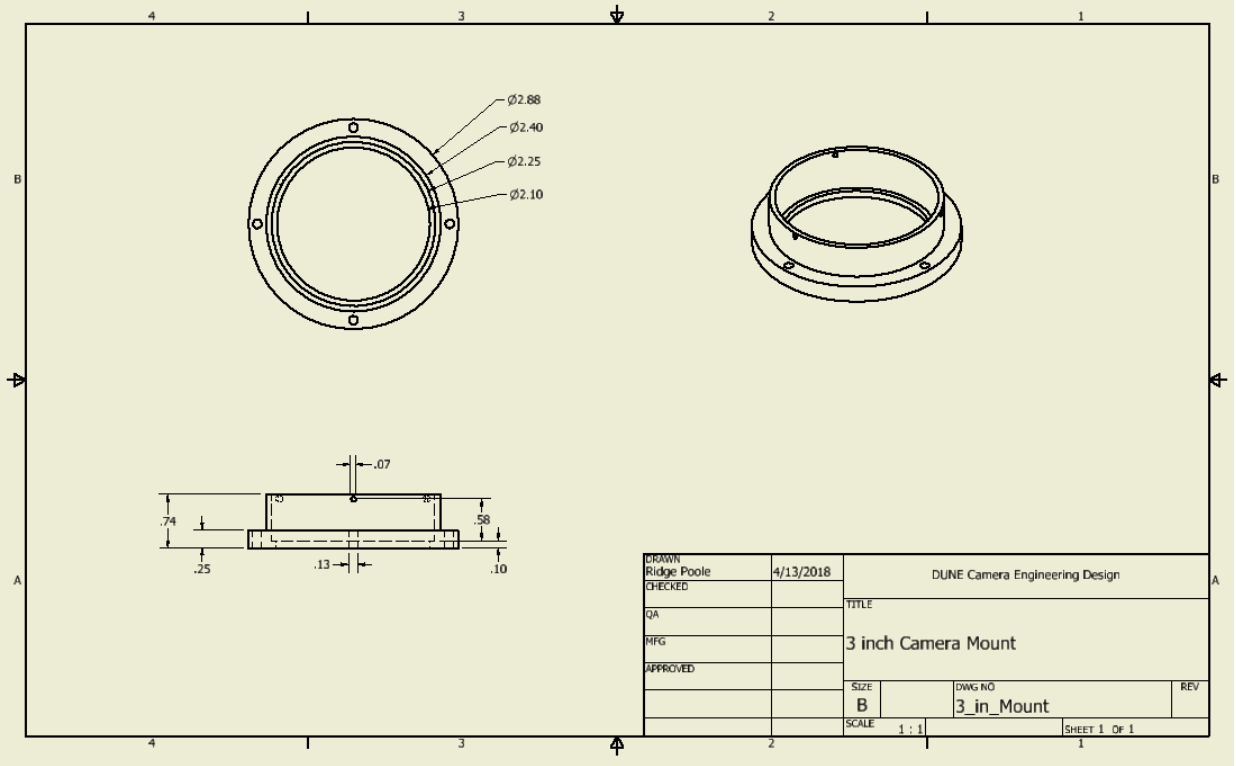
Ø2.88
Ø2.40
Ø2.25
Ø2.10
.07
.74
.58
.25
.13
.10
DRAWN
Ridge Poole
4/13/2018
CHECKED
QA
MFG
APPROVED
DUNE Camera Engineering Design
TITLE
3 inch Camera Mount
SIZE
B
DWG NO
3_in_Mount
REV
SCALE
1 : 1
SHEET 1 OF 1

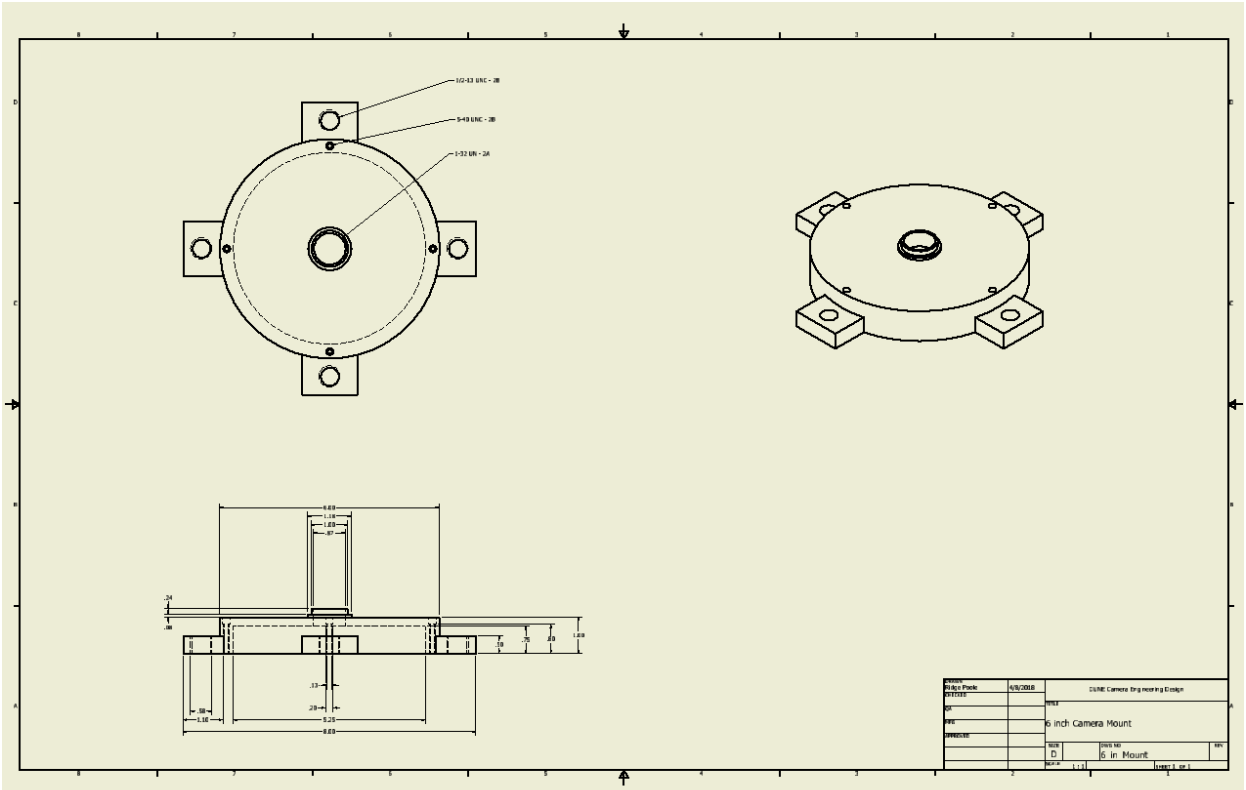
1/2-13 UNC - 2B
5-40 UNC - 2B
1-32 UN - 2A
6 inch Camera Mount
6 in Mount

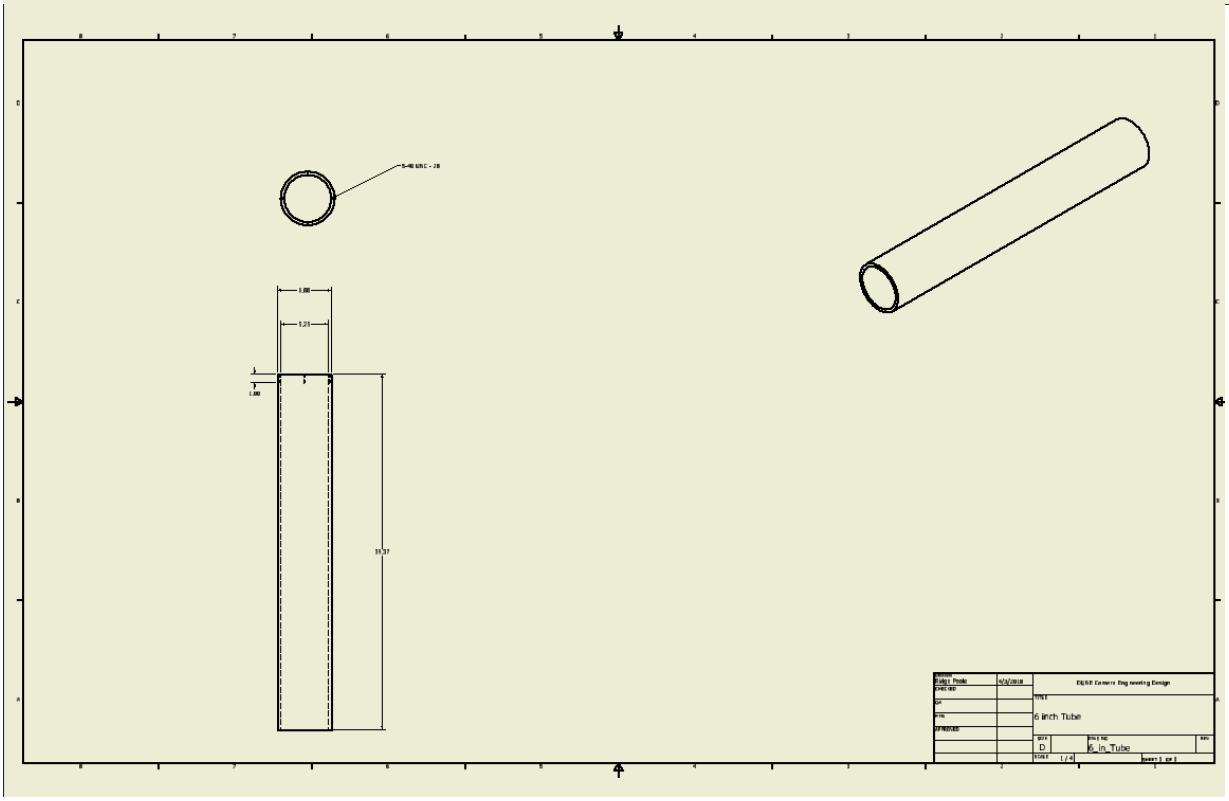
5-40 UNC - 2B
6 inch Tube
6_in_Tube

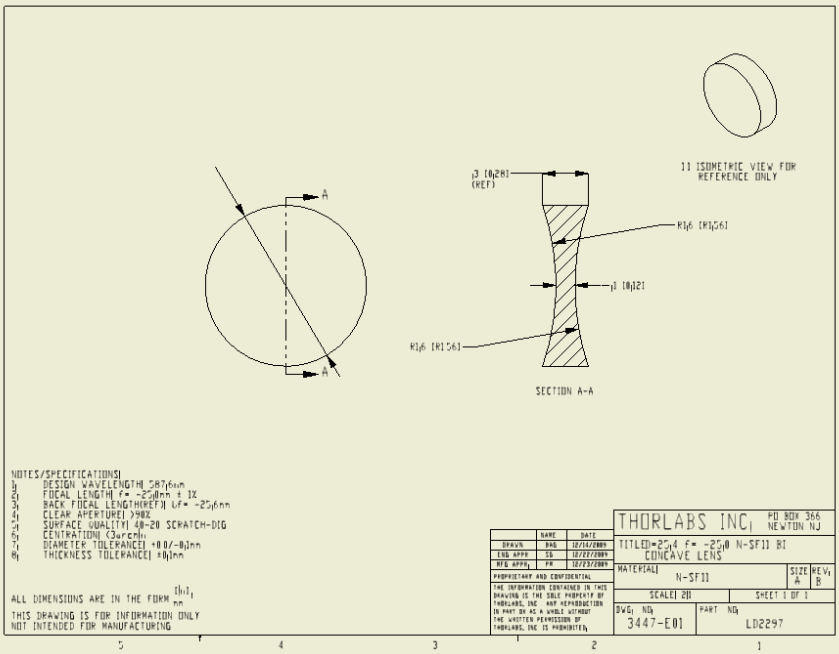
11 ISOMETRIC VIEW FOR REFERENCE ONLY
3 [0,28] (REF)
Ry6 [R1,56]
1 [0,12]
Ry6 [R1,56]
SECTION A-A
NOTES/SPECIFICATIONS:
1: DESIGN WAVELENGTH: 587.6nm
2: FOCAL LENGTH: f= -25.0mm ± 1%
3: BACK FOCAL LENGTH(REF): bf= -23.6mm
4: CLEAR APERTURE: >90%
5: SURFACE QUALITY: 40-20 SCRATCH-DIG
6: CENTRATION: 3 arcmin
7: DIAMETER TOLERANCE: +0.0/-0.1mm
8: THICKNESS TOLERANCE: ±0.1mm
ALL DIMENSIONS ARE IN THE FORM [in] / [mm]
THIS DRAWING IS FOR INFORMATION ONLY
NOT INTENDED FOR MANUFACTURING
NAME DATE
DRAWN BMG 12/14/2009
ENG APPR. TS 12/22/2009
MFG APPR. PR 12/23/2009
PROPRIETARY AND CONFIDENTIAL
THE INFORMATION CONTAINED IN THIS DRAWING IS THE SOLE PROPERTY OF THORLABS, INC AND REPRODUCTION IN PART OR AS A WHOLE WITHOUT THE WRITTEN PERMISSION OF THORLABS, INC IS PROHIBITED.
THORLABS INC. PO BOX 366 NEWTON NJ
TITLE: 25.4 f= -25.0 N-SF11 BI CONCAVE LENS
MATERIAL: N-SF11
SIZE A REV: B
SCALE: 2:1
SHEET 1 OF 1
DWG. NO. 3447-E01
PART NO. LD2297

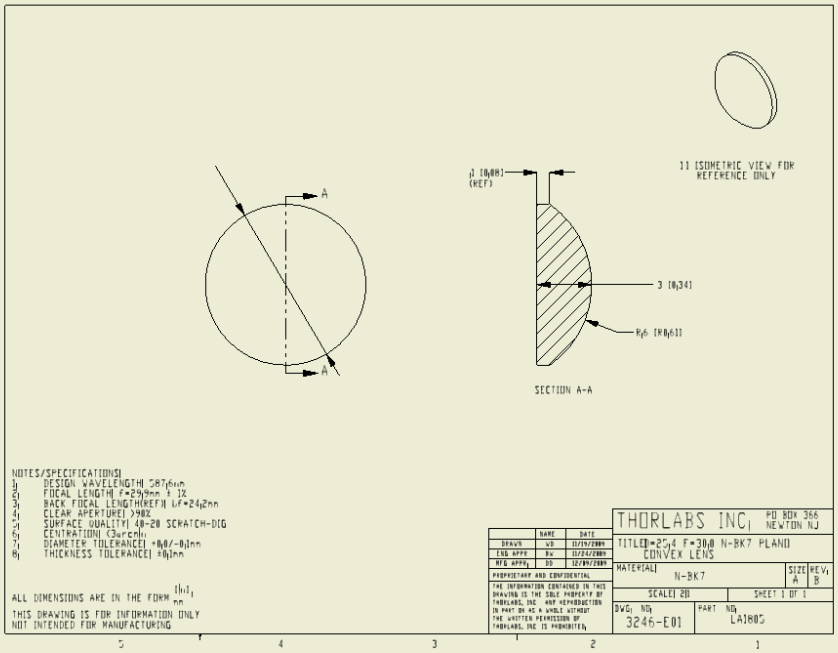
11 ISOMETRIC VIEW FOR REFERENCE ONLY
1 [0,08] (REF)
3 [0,34]
Ry6 [R0,61]
SECTION A-A
NOTES/SPECIFICATIONS:
1: DESIGN WAVELENGTH: 587.6nm
2: FOCAL LENGTH: f=29.9mm ± 1%
3: BACK FOCAL LENGTH(REF): bf=24.2mm
4: CLEAR APERTURE: >90%
5: SURFACE QUALITY: 40-20 SCRATCH-DIG
6: CENTRATION: 3 arcmin
7: DIAMETER TOLERANCE: +0.0/-0.1mm
8: THICKNESS TOLERANCE: ±0.1mm
ALL DIMENSIONS ARE IN THE FORM [in] / [mm]
THIS DRAWING IS FOR INFORMATION ONLY
NOT INTENDED FOR MANUFACTURING
NAME DATE
DRAWN WB 11/19/2009
ENG APPR. BW 11/24/2009
MFG APPR. DD 12/09/2009
PROPRIETARY AND CONFIDENTIAL
THE INFORMATION CONTAINED IN THIS DRAWING IS THE SOLE PROPERTY OF THORLABS, INC AND REPRODUCTION IN PART OR AS A WHOLE WITHOUT THE WRITTEN PERMISSION OF THORLABS, INC IS PROHIBITED.
THORLABS INC. PO BOX 366 NEWTON NJ
TITLE: 25.4 F=30.0 N-BK7 PLANO CONVEX LENS
MATERIAL: N-BK7
SIZE A REV: B
SCALE: 2:1
SHEET 1 OF 1
DWG. NO. 3246-E01
PART NO. LA1805

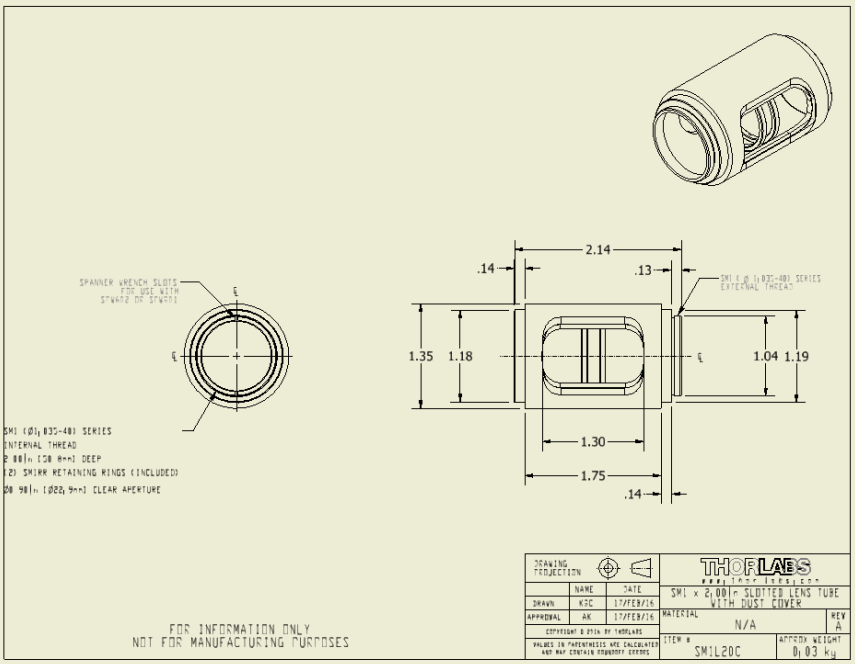
SPANNER WRENCH SLOTS
FOR USE WITH
SPW402 OR SPW701
SM1 (Ø1.035-40) SERIES
INTERNAL THREAD
2.00in (50.8mm) DEEP
(2) SMRR RETAINING RINGS (INCLUDED)
Ø0.98in (Ø22.9mm) CLEAR APERTURE
2.14
.14
.13
SM1 (Ø1.035-40) SERIES
EXTERNAL THREAD
1.35
1.18
1.04
1.19
1.30
1.75
.14
FOR INFORMATION ONLY
NOT FOR MANUFACTURING PURPOSES
DRAWING PROJECTION
NAME
DATE
DRAWN
KSC
17/FEB/15
APPROVAL
AK
17/FEB/15
COPYRIGHT & 2016 BY THORLABS
VALUES IN PARENTHESIS ARE CALCULATED AND MAY CONTAIN ROUNDOFF ERRORS
THORLABS
www.thorlabs.com
SM1 x 2.00in SLOTTED LENS TUBE WITH DUST COVER
MATERIAL
N/A
REV
A
ITEM #
SM1L20C
APPROX. WEIGHT
0.03 kg

Bibliography

[1] Deep Underground Neutrino Experiment. (2018). Neutrino Detectors. Retrieved Fall, 2017, from http://www.dunescience.org/neutrino-detectors/

[2] Ibid

[3] Deep Underground Neutrino Experiment. (2018). An international mega-science project. Retrieved Fall, 2017, from http://www.dunescience.org/

[4] Fermilab. (2016, November 1). Long-Baseline Neutrino Facility (LBNF). Retrieved Fall, 2017, from https://lbnf.fnal.gov/cryo.html

[5] Deep Underground Neutrino Experiment. (2018). Why Neutrinos. Retrieved Fall, 2017, from http://www.dunescience.org/why-neutrinos/

[6] Ibid

[7] Fermilab. (2018, March 13). NOvA Neutrino Experiment. Retrieved Fall, 2017, from https://www-nova.fnal.gov/

[8] MINERvA at Fermilab. (2015, March). MINERvA: Bringing Neutrinos into Sharp Focus. Retrieved Fall, 2017, from https://minerva-exp.fnal.gov/

[9] Brunetti, G. (2017, March 16). *Dual-Phase Liquid Argon Time Projection Chambers* [PPT]. Fermilab.

[10] Edmund Optics Worldwide. (2018). Understanding Focal Length and Field of View | Edmund Optics. Retrieved Spring, 2018, from https://www.edmundoptics.com/resources/application-notes/imaging/understanding-focal-length-and-field-of-view

[11] Airgas: an Air Liquide Company. (2018). Products: Industrial Application Gases. Retrieved Spring, 2018, from http://www.airgas.com/category/Gases-Industrial-Application-Gases

[12] RefractiveIndex.Info. (2008-2018). Refractive Index Database. Retrieved Fall, 2017, from https://refractiveindex.info